Semiconductors: a μSR approach

A SEMI-CONDUCTOR

Peter Y. Yu Manuel Cardona Fundamentals of Semiconductors

Outline

1. Why semiconductors?
2. Hydrogen: an ubiquitous impurity
   a) Using muonium as a light pseudo-isotope of H
   b) "Typical example": Si
   c) Complementarity to other techniques
   d) H/Muonium impurity levels
   e) Diffusion and passivation
3. Probing other defects
   a) H passivation
   b) Defect layers
4. Adressing charge carrier dynamics

1. Why semiconductors?

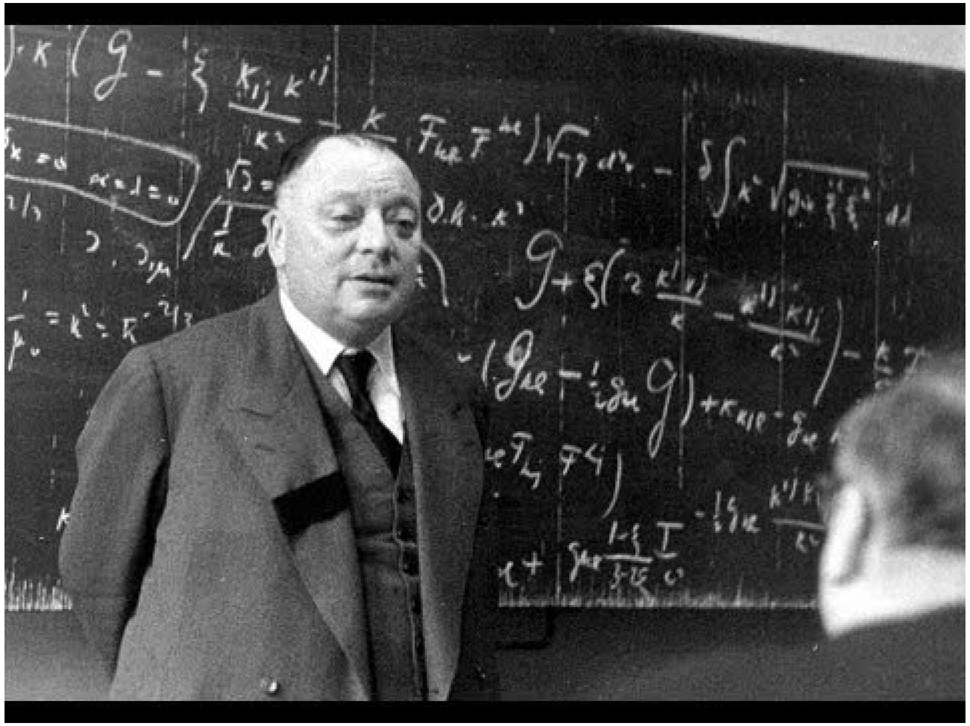

"Über Halbleiter soll man nicht arbeiten, das ist eine Schweinerei; wer weiss, ob es überhaupt Halbleiter gibt."

Wolfgang Pauli, Letter to Peierls, 29 September 1931
Wolfgang Pauli – Wissenschaftlicher Briefwechsel mit Bohr, Einstein, Heisenberg u.a. Band II: 1930–1939, Springer, 1985, p. 94

"One shouldn't work on semiconductors, that is a filthy mess; who knows whether any semiconductors exist."

1. Why semiconductors?

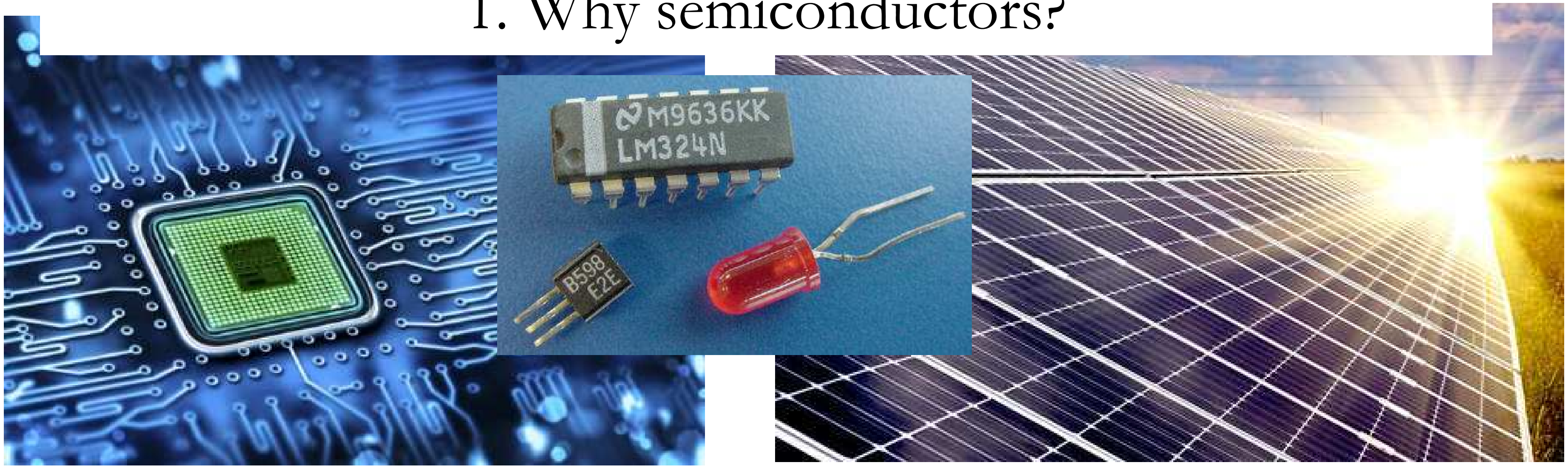

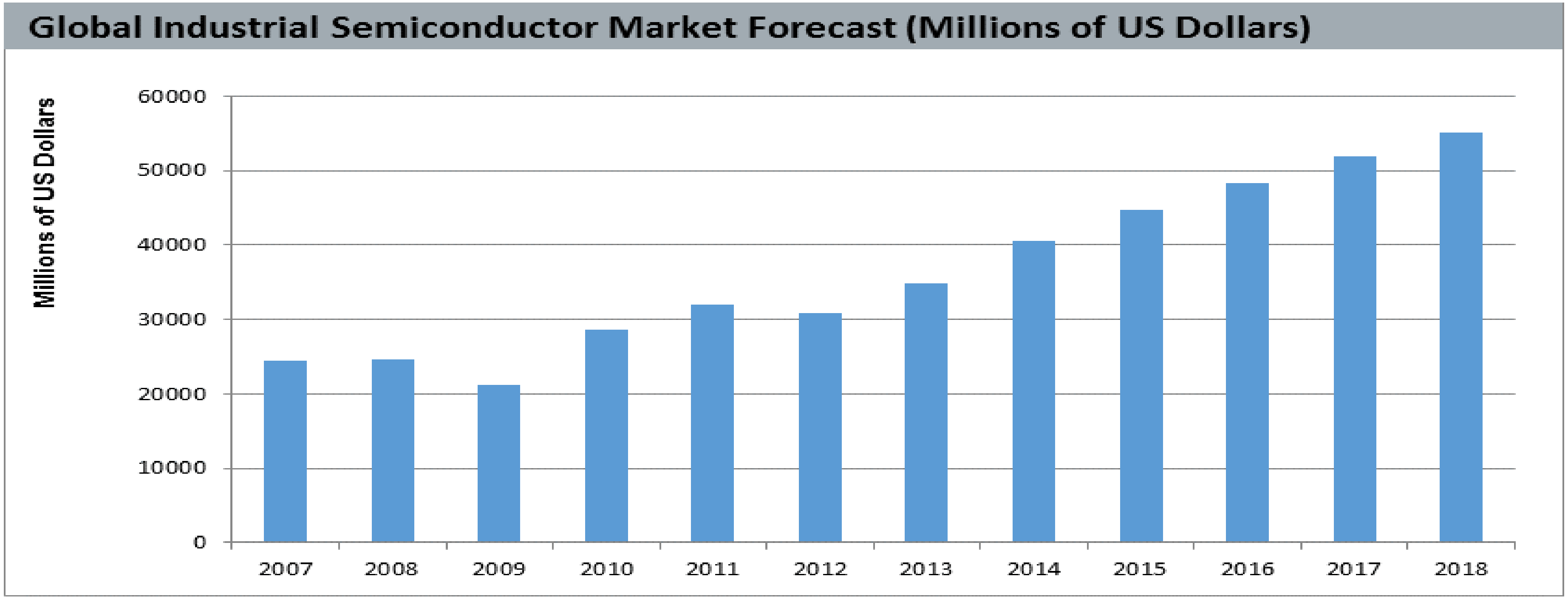

Source: http://news.ihsmarkit.com/press-release/technology/recovering-economies-driving-growth-industrial-semiconductor-market-ihs-say

Reminder: from atomic levels to energy bands in solids

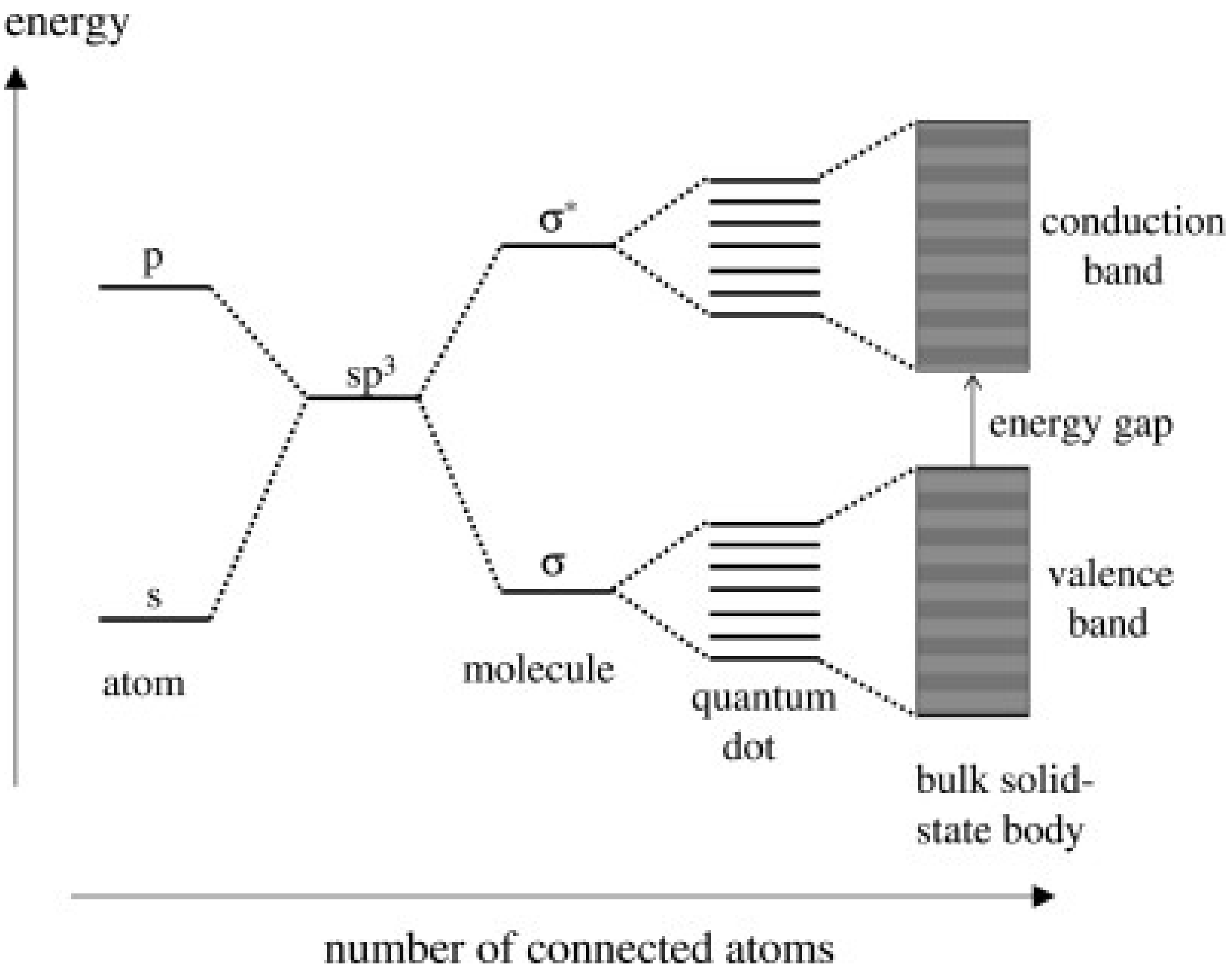

Parak, W. J., Manna, L. and Nann, T. 2010. Fundamental Principles of Quantum Dots. Nanotechnology. 1:4:73–96.

Reminder: metals and semimetals, insulators and semiconductors

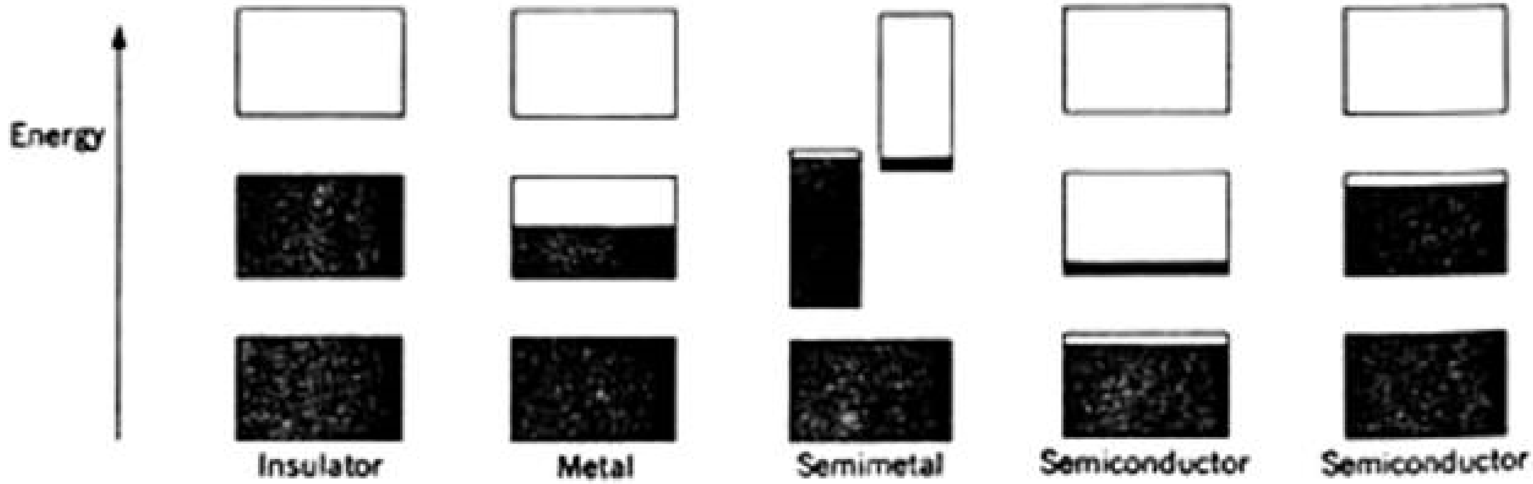

Figure 1 Schematic electron occupancy of allowed energy bands for an insulator, metal, semimetal, and semiconductor. The vertical extent of the boxes indicates the allowed energy regions; the shaded areas indicate the regions filled with electrons. In a **semimetal** (such as bismuth) one band is almost filled and another band is nearly empty at absolute zero, but a pure **semiconductor** (such as silicon) becomes an insulator at absolute zero. The left of the two semiconductors shown is at a finite temperature, with carriers excited thermally. The other semiconductor is electron-deficient because of impurities.

C. Kittel, Solid State Physics

Semiconductors: it's all about impurities and defects!

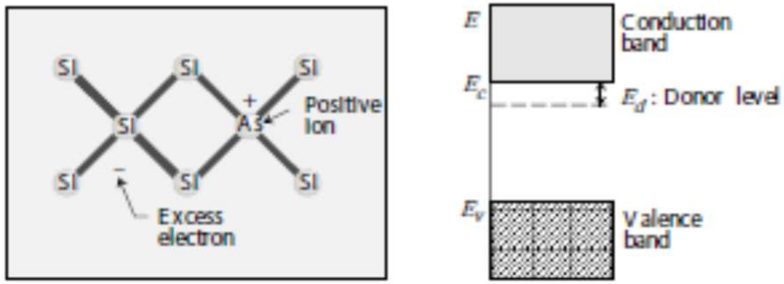

Arsenic (As) atom donates one electron to the conduction band to produce an *n*-type silicon

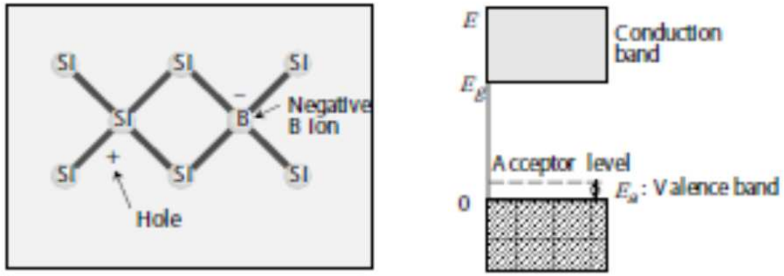

One electron taken from the valence band to complete the bonding of the boron atom → hole

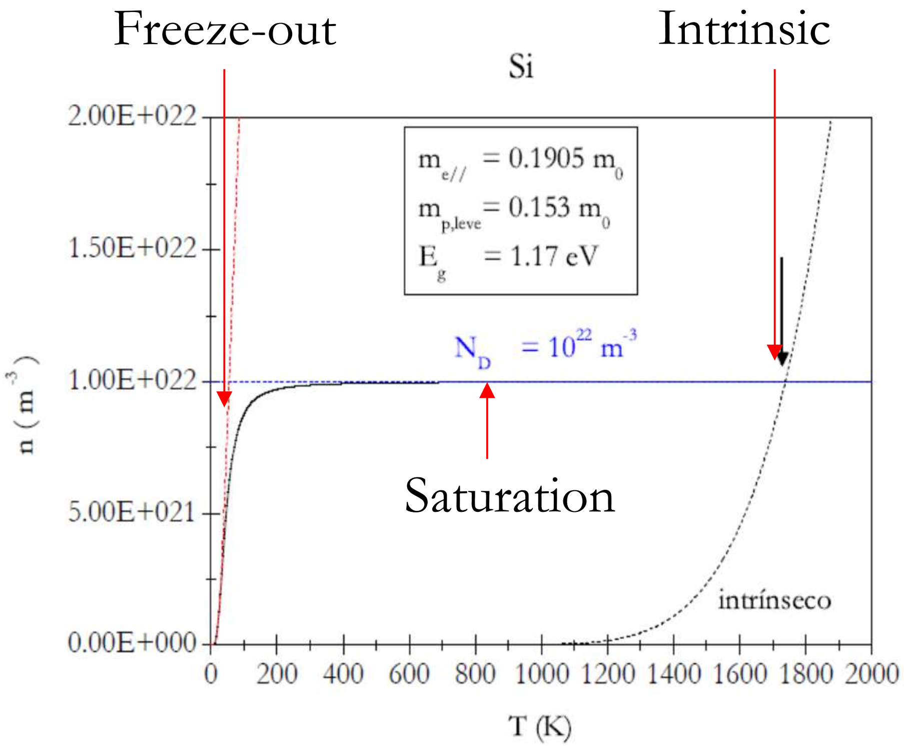

2. Hydrogen, an omnipresent impurity

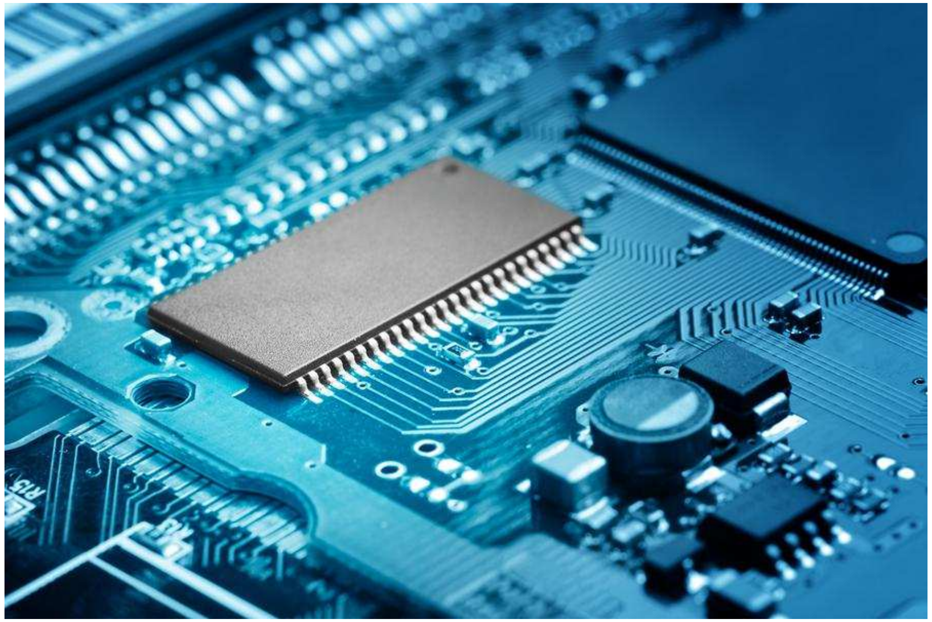

Hydrogen can be incorporated in semiconductor materials and semiconductor devices in many of the fabrication steps, from initial growth conditions to ageing of fully developed devices.

Interaction of hydrogen with impurities/defects

...mostly passivating other impurities/defects

Appl. Phys. Lett. 32(12), 15 June 1978

Photoluminescence recovery in rehydrogenated amorphous silicon[a)]

J. I. Pankove

RCA Laboratories, Princeton, New Jersey 08540

(Received 20 February 1978; accepted for publication 21 March 1978)

The rehydrogenation of thermally dehydrogenated amorphous silicon restores the luminescence characteristics of a-Si:H.

PACS numbers: 78.55.Ds, 81.40.Tv

Passivation of dangling bonds in amorphous silicon, removing unwanted levels (charge-carrier traps) from the band gap

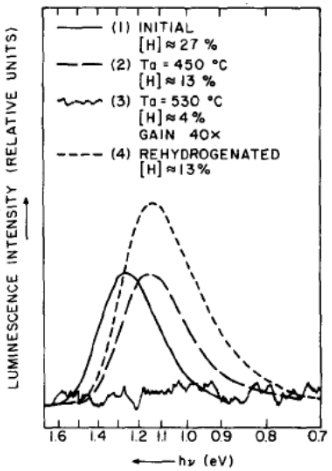

FIG. 1. Photoluminescence spectra of a-Si:H at 79 °K. Excitation: 50 mW at 488 nm from an argon laser; detection: cooled PbS photoconductor.

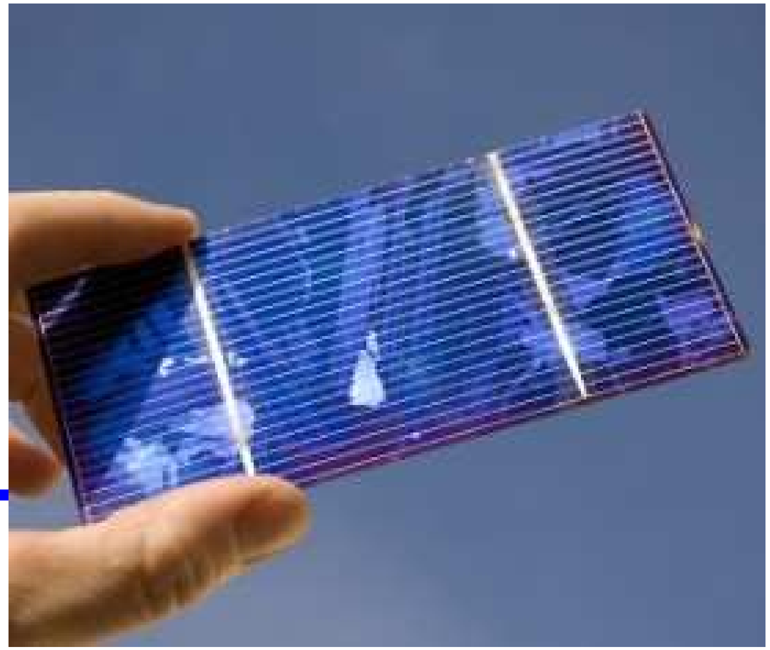

Identification of H as responsible for passivation of Mg acceptors in GaN was a crucial step in the devellopment of blue LEDs (Nobel Prize in Physics 2014)

S. Nakamura *et al.*,
Jpn. J. Appl. Phys. **31**, 1258 (1992)

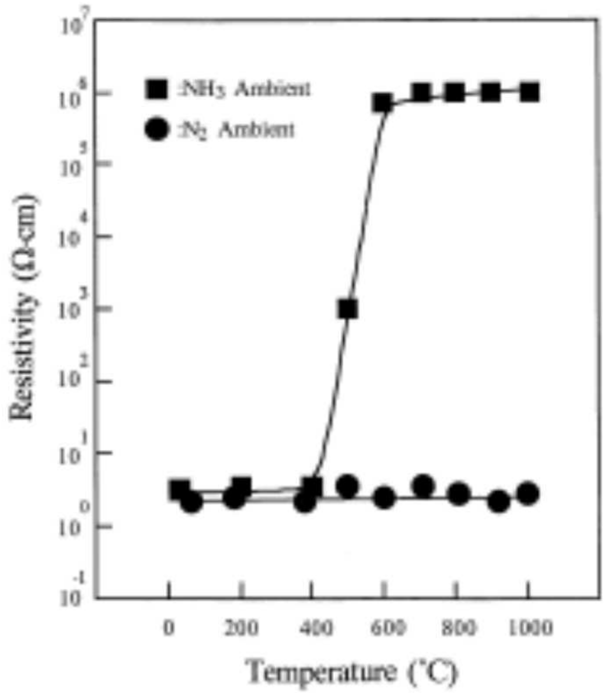

Fig. 1. The resistivity change in LEEBI-treated Mg-doped GaN films as a function of annealing temperature. The ambient gases, NH_3 and N_2, were used for thermal annealing.

Press Release

7 October 2014

The Royal Swedish Academy of Sciences has decided to award the Nobel Prize in Physics for 2014 to

Isamu Akasaki
Meijo University, Nagoya, Japan and Nagoya University, Japan

Hiroshi Amano
Nagoya University, Japan

and

Shuji Nakamura
University of California, Santa Barbara, CA, USA

"for the invention of efficient blue light-emitting diodes which has enabled bright and energy-saving white light sources"

When isolated, H is most commonly a compensating impurity

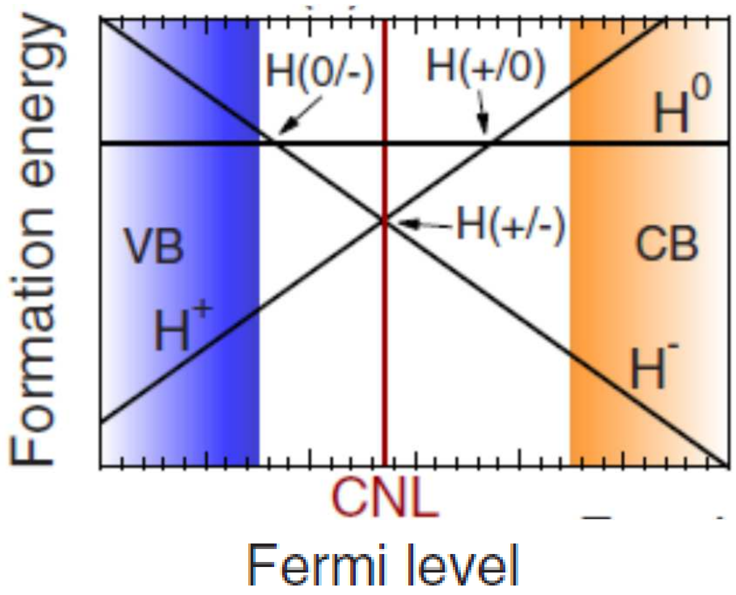

Donor state H^+ is stable in p-type material and acceptor H^- is stable in n-type material

Compensating H helps keeping the insulating character of high-k dielectric oxides used in the gates of MOSFET devices

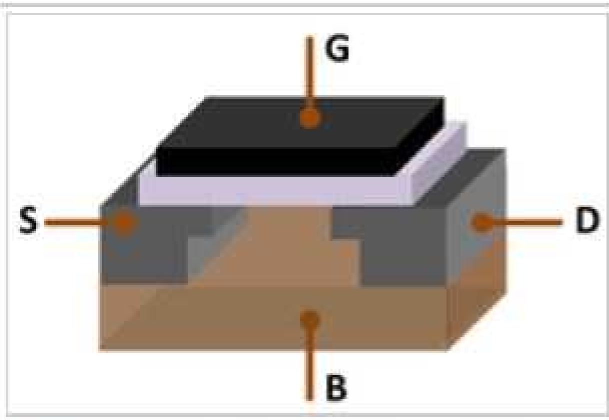

MOSFET showing gate (G), body (B), source (S) and drain (D) terminals. The gate is separated from the body by an insulating layer (white)

Passivation? Compensation? What is the difference?

Compensation: both impurities/defects are isolated from each other, but the respective contributions to conductivity are opposite.

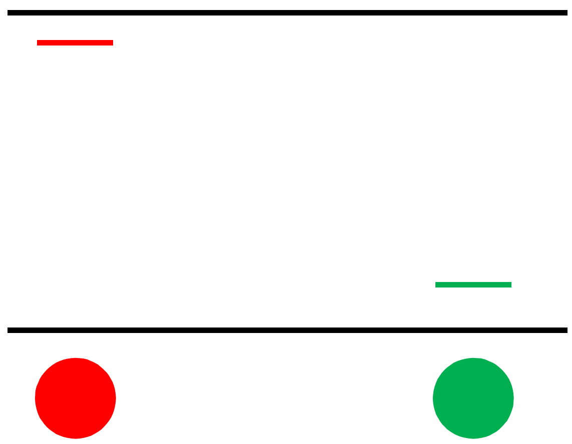

Passivation: neutralization of the electrical behaviour of an impurity/defect by formation of a complex with another impurity/defect.

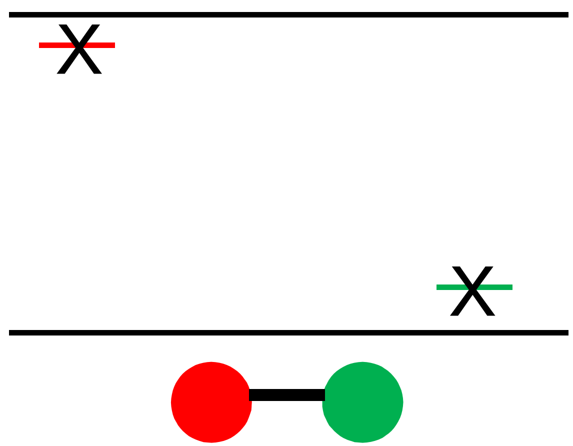

Passivation and compensation can be distinguished by transport measurements.

H can be electrically active in some cases

Donor state H^+ is the stable state independently of doping.

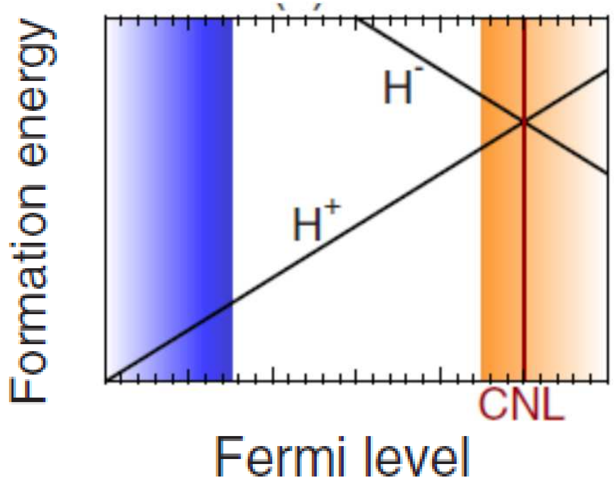

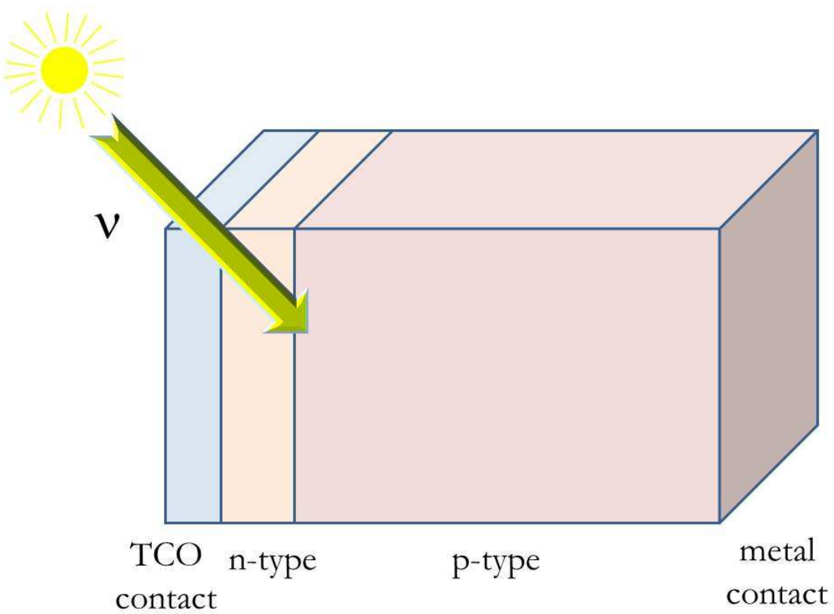

H is a candidate dopant for transparent conductive oxides

A key to the problem: band line-ups

CG Van de Walle and J. Neugebauer,
Nature **423** (2003)

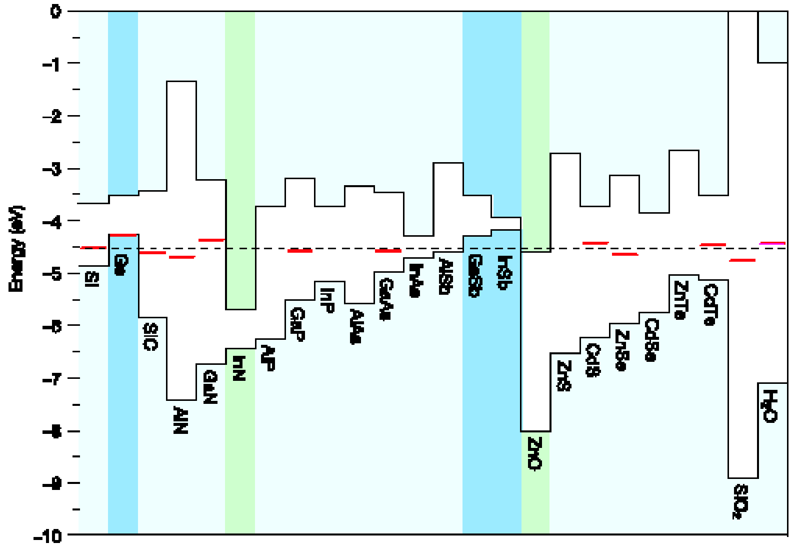

Ç Kiliç and A Zunger,
App. Phys. Lett. **81,** 73 (2002)

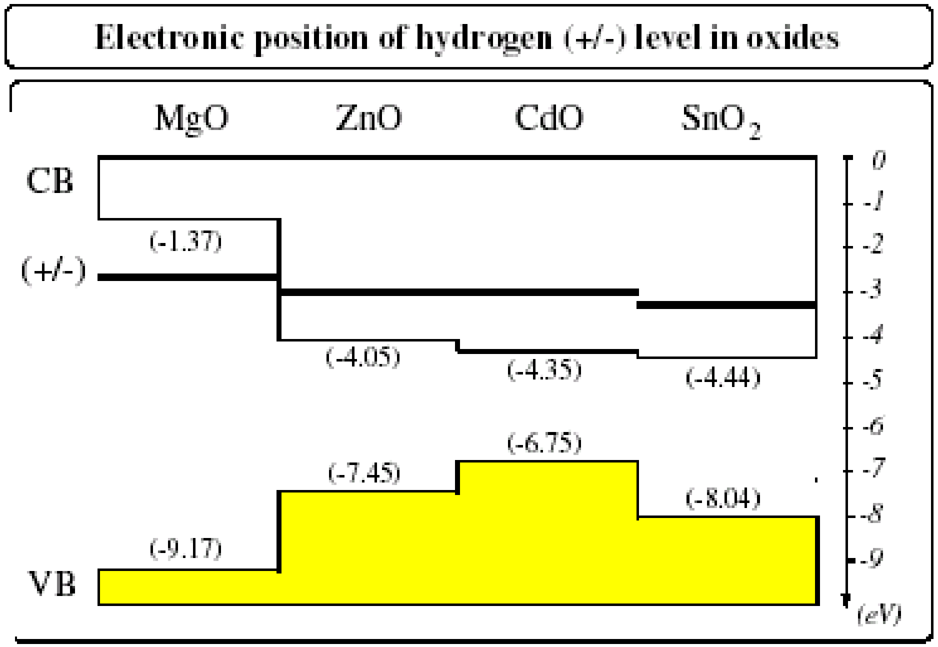

$\varepsilon(+/-)$ predicted to be constant

However, isolated H is an elusive species

High-concentrations of H are typically required for detection.

The use of experimental techniques sensitive to isolated hydrogen itself is limited to a couple of systems where hydrogen is usually present in high concentrations (notably ZnO and TiO_2).

Microscopic information about isolated hydrogen configurations, electronic structure and electronic levels is even more difficult to obtain.

Most information about isolated H comes from muSR.

2 a) Using Mu as a light pseudo-isotope of hydrogen

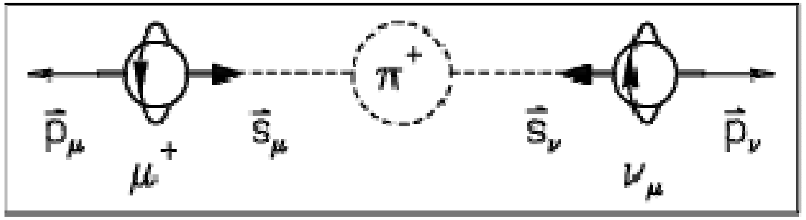

$$\mu^+ \xrightarrow[2.2\,\mu s]{} e^+ + \overline{\nu}_\mu + \nu_e$$

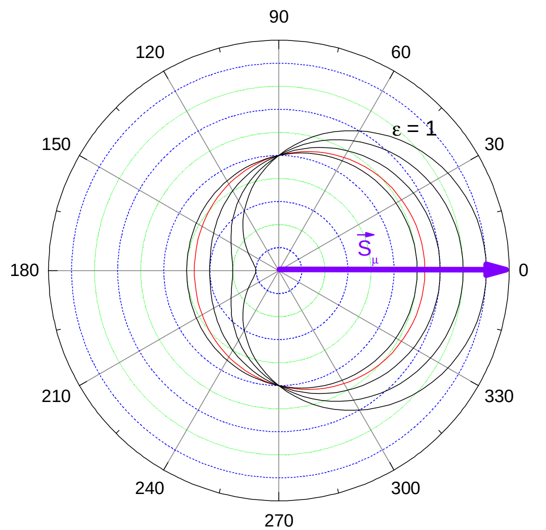

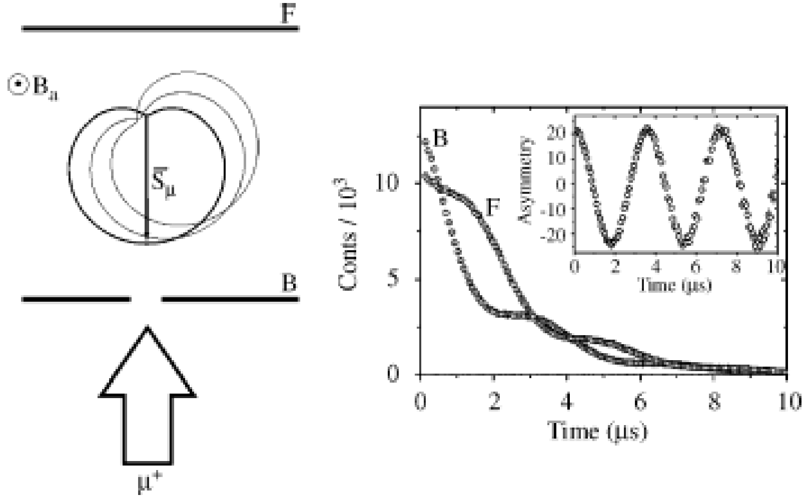

Using Mu as a light pseudo-isotope of hydrogen

Mu: bound state of e^- and μ^+ Mu= [$e^- \mu^+$]

	Mu	H
Reduced mass (m_e)	0.995187	0.999456
Binding energy in the ground state (eV)	13.54	13.60
Hyperfine parameter (MHz)	4463	1420.4
Gyromagnetic ratio/ (MHz T^{-1})	135.54	42.58
Atomic radius in the ground state (Å)	0.531736	0.529465

$$A \propto \mu_{nucleus} |\Psi_{1s}(r=0)|^2$$

$$\frac{A_{Mu}}{A_H} \sim \frac{\mu_{Mu}}{\mu_H} \Longrightarrow |\Psi_{1s}(r=0)|^2{}_{Mu} \sim |\Psi_{1s}(r=0)|^2{}_H$$

What about isotopic effects?

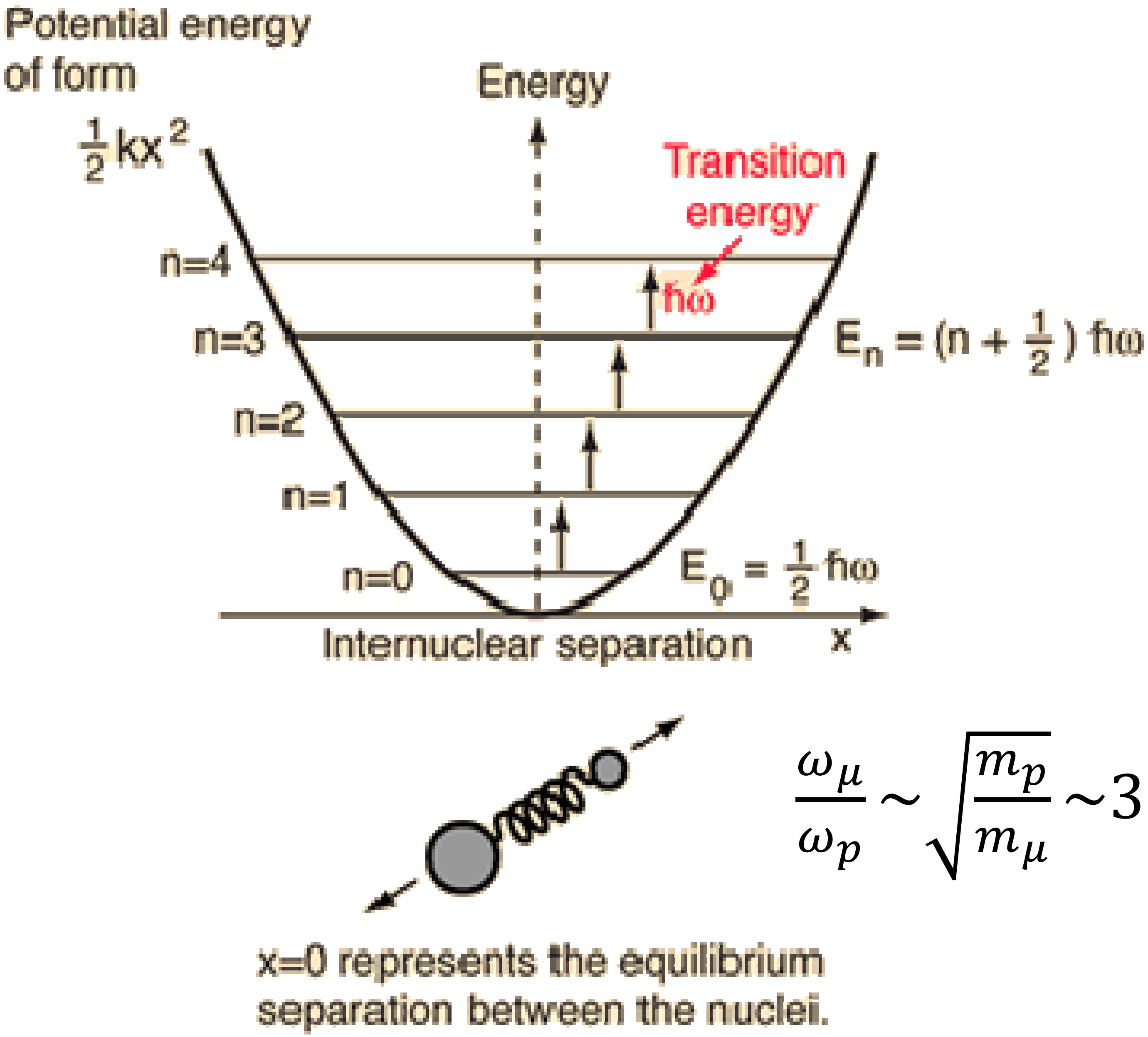

$$\omega = \sqrt{\frac{k}{m}}$$

$$\frac{\omega_\mu}{\omega_p} \sim \sqrt{\frac{m_p}{m_\mu}} \sim 3 \Rightarrow \omega_\mu \sim 3\omega_p$$

Isotropic "normal" muonium

$$H = hA\mathbf{S}_\mu \cdot \mathbf{S}_e - \frac{g_\mu \mu_\mu B}{\hbar}\hat{\mathbf{S}}_{\mu,z} + \frac{g_e \mu_B B}{\hbar}\hat{\mathbf{S}}_{e,z} = hA\mathbf{S}_\mu \cdot \mathbf{S}_e - \omega_\mu \hat{\mathbf{S}}_{\mu,z} + \omega_e \hat{\mathbf{S}}_{e,z}$$

hyperfine interaction

muon and electron
Zeeman interactions

$$A = \frac{\mu_0}{4\pi}\frac{8}{3}\frac{g_\mu \mu_\mu g_e \mu_B}{a_0^3} = \frac{\mu_0}{4\pi}\frac{8\pi}{3} g_\mu \mu_\mu g_e \mu_B \left|\Psi_{1s}(r=0)\right|^2$$

$$\omega_e = 2\pi\gamma_e B$$

$$\omega_\mu = 2\pi\gamma_\mu B$$

$$\gamma_\mu = g_\mu \mu_\mu / h = 135.53\,\mathrm{MHz/T}$$

$$\gamma_e = g_e \mu_B / h = 28024.21\,\mathrm{MHz/T}$$

Small magnetic fields: hyperfine interaction dominates

spins add up to a total spin F=1, yielding a triplet $F = 1$ state with energy $h\,A/4$

$$|1\rangle = |++\rangle = |F = 1, m_F = +1\rangle$$

$$|2\rangle = \frac{\sqrt{2}}{2}|+-\rangle + \frac{\sqrt{2}}{2}|-+\rangle = |F = 1, m_F = 0\rangle$$

$$|3\rangle = |--\rangle = |F = 1, m_F = -1\rangle$$

and a singlet $F = 0$ state with energy $-3\,h\,A/4$

$$|4\rangle = \frac{\sqrt{2}}{2}|+-\rangle - \frac{\sqrt{2}}{2}|-+\rangle = |F = 0, m_F = 0\rangle$$

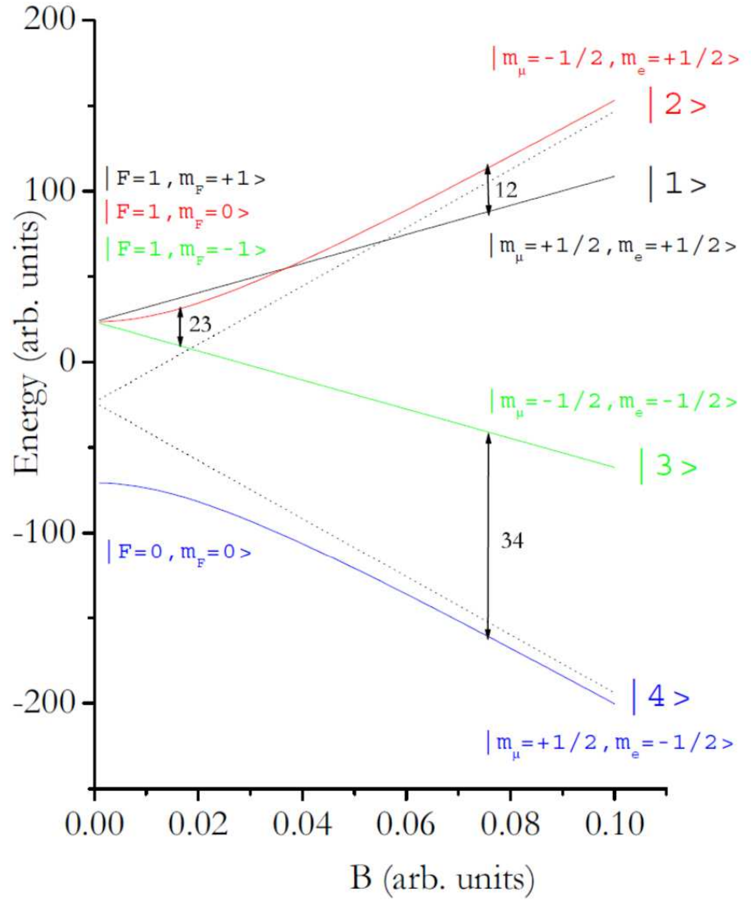

Figure 2.1: Energy eigenvalues of the isotropic muonium hyperfine hamiltonian 2.3, as a function of the applied magnetic field B. This diagram is usually known as the Breit-Rabi diagram. We have used a fictitious value of γ_e ($\gamma_e = 3\gamma_\mu$), in order to display more clearly the essential features of this diagram. We draw as well, as dashed lines, the asymptotes of the non-linear eigenenergies of the $|2\rangle$ and $|4\rangle$ eigenstates.

High magnetic fields: Zeeman interactions dominate

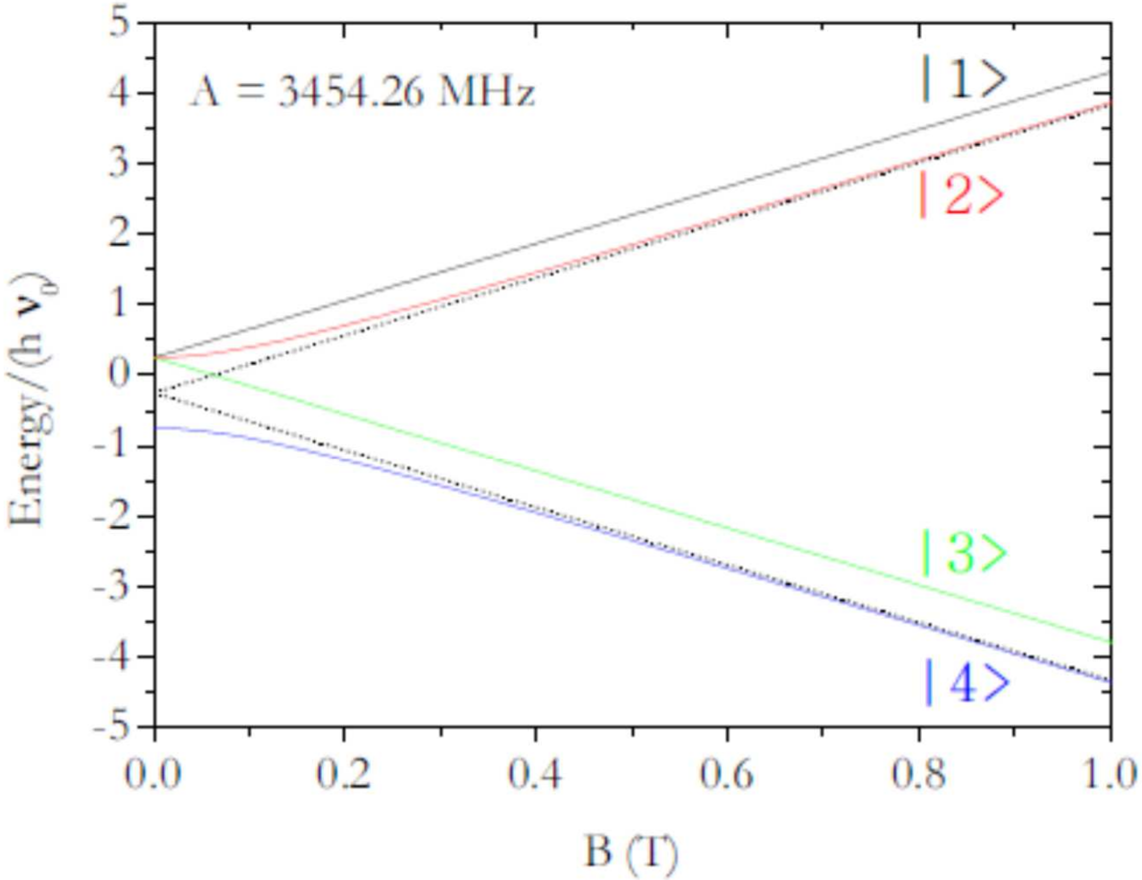

$$|1\rangle \rightarrow |++\rangle$$
$$|2\rangle \rightarrow |-+\rangle$$
$$|3\rangle \rightarrow |--\rangle$$
$$|4\rangle \rightarrow |+-\rangle$$

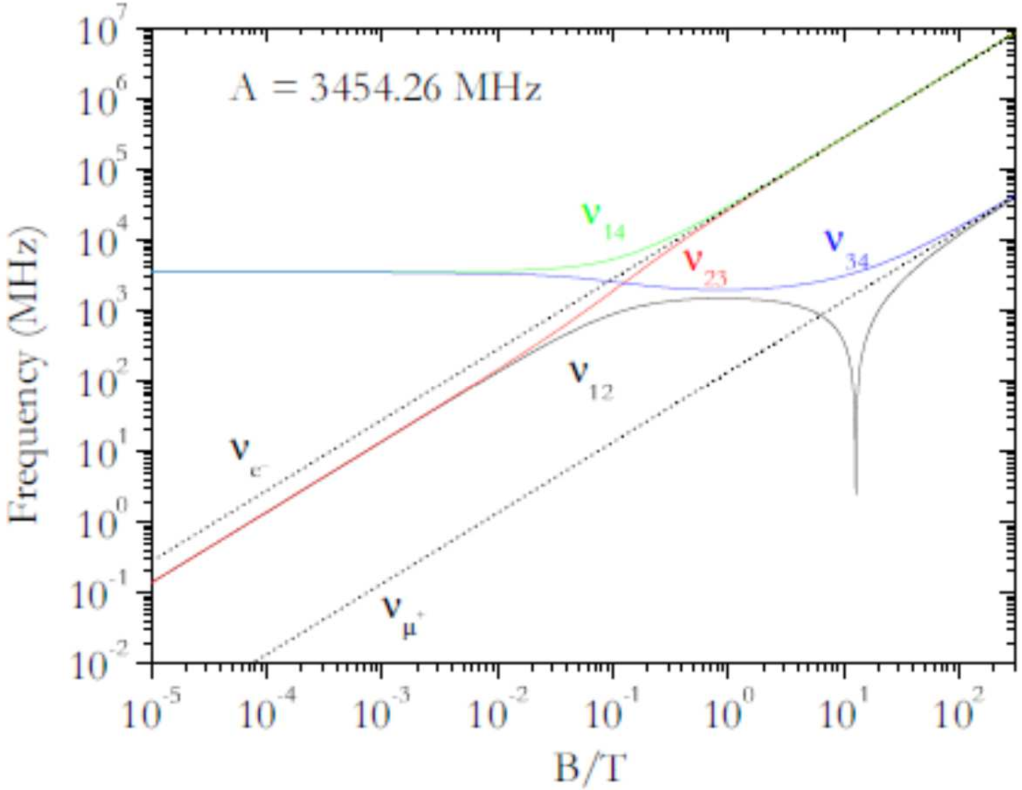

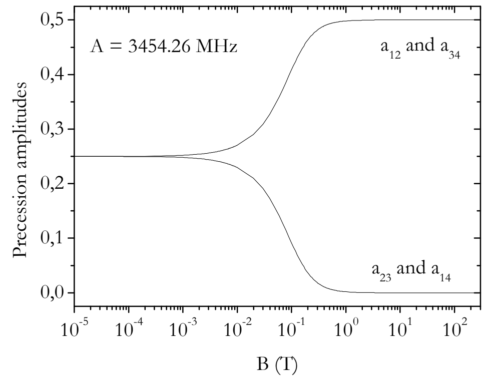

In the high-field limit, we have

$$\nu_{12} \rightarrow \gamma_\mu B - \frac{A}{2}$$
$$\nu_{14} \rightarrow \gamma_e B + \frac{A}{2}$$
$$\nu_{23} \rightarrow \gamma_e B - \frac{A}{2}$$
$$\nu_{34} \rightarrow \gamma_\mu B + \frac{A}{2}$$

2 b) Hydrogen/Mu in Si: the classical example

Muonium was first identified in Si by longitudinal-field quenching

PHYSICAL REVIEW VOLUME 107, NUMBER 5 SEPTEMBER 1, 1957

Paschen-Back Effect as a Means of Detecting Muonium*

RICHARD A. FERRELL AND FERNANDO CHAOS†
University of Maryland, College Park, Maryland
(Received May 24, 1957)

PHYSICAL REVIEW VOLUME 118, NUMBER 1 APRIL 1, 1960

Magnetic Quenching of Hyperfine Depolarization of Positive Muons*

R. A. FERRELL, Y. C. LEE, AND M. K. PAL†
University of Maryland, College Park, Maryland
(Received August 24, 1959)

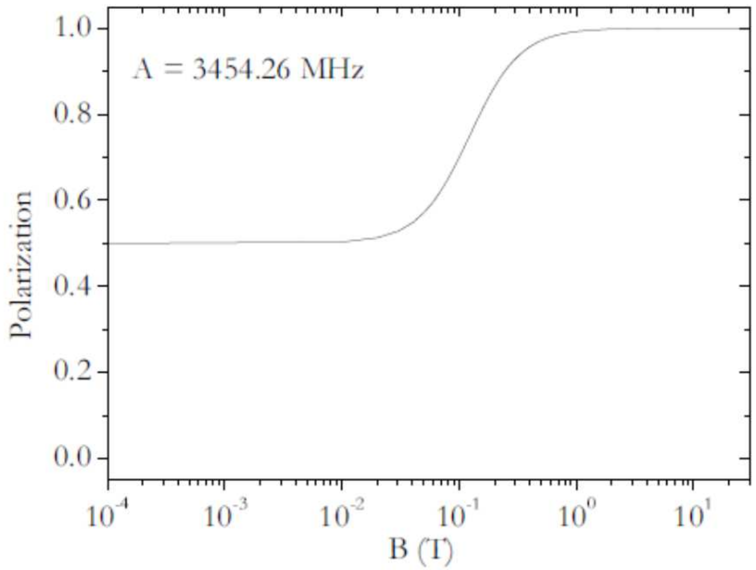

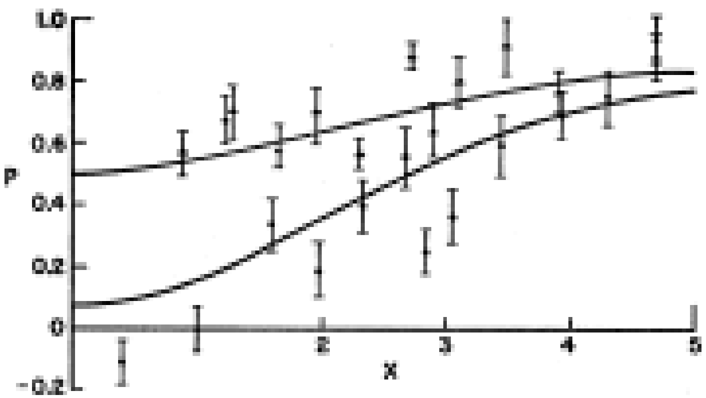

FIG. 1. Dependence of muon polarization P on magnetic field x, measured in units of 1.58 kilogauss. The magnetic quenching data shown are those of Sens et al. (reference 6) for nuclear emulsion (triangles) and fused quartz (circles). The fits achieved by the present theory, which takes into account the finite lifetime of the muonium atom with respect to breakup, are given by the upper and lower curves (nuclear emulsion and fused quartz, respectively).

$$p = a_{\parallel} = \frac{1}{2} + \frac{x^2}{2\left(1 + x^2\right)}$$

The spectroscopic measurements had a surprise:

PHYSICAL REVIEW LETTERS

VOLUME 31 | 16 JULY 1973 | NUMBER 3

Anomalous μ^+ Precession in Silicon*

J. H. Brewer, K. M. Crowe, F. N. Gygax,† R. F. Johnson, and B. D. Patterson
Lawrence Berkeley Laboratory, University of California, Berkeley, California 94720

and

D. G. Fleming
University of British Columbia, Vancouver, Canada

and

A. Schenck
Institut für Hochenergiephysik, Eidgenössische Technische Hochschule, Zürich, c/o Schweizerisches Institut für Nuklearforschung, Villigen, Switzerland

(Received 27 April 1973)

We have studied precession of polarized positive muons in quartz and silicon in transverse magnetic fields, via the asymmetric decay. We observed free muon precession and two-frequency muonium precession, as well as two anomalous precession frequencies apparent only in silicon.

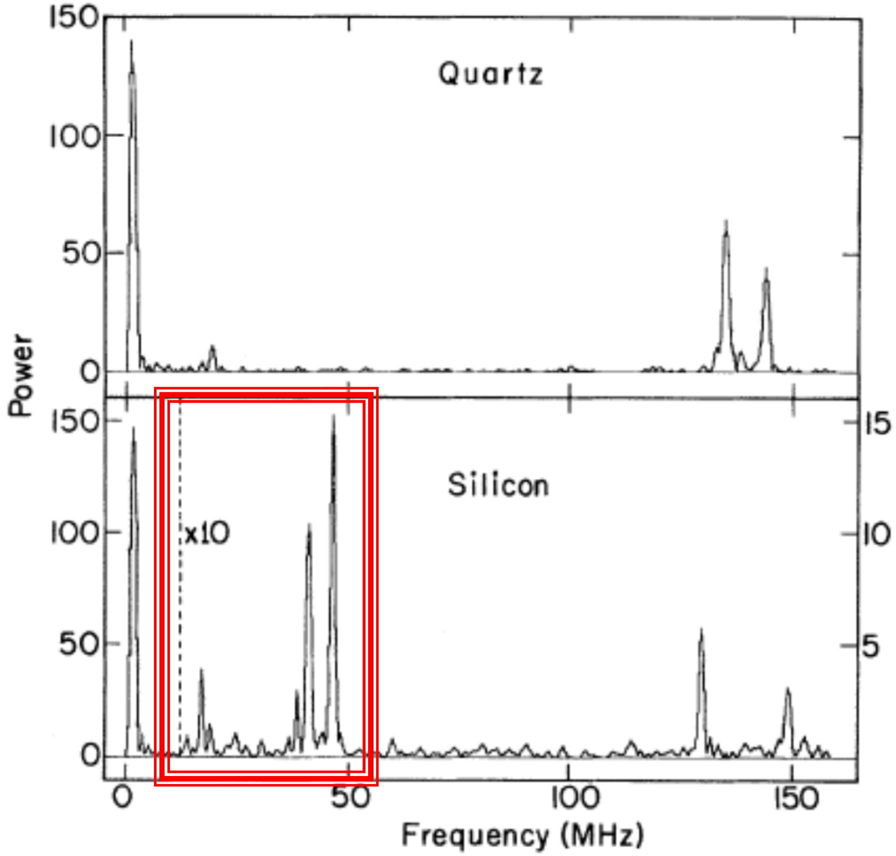

Anisotropic "anomalous" muonium

$$H = h\,\mathbf{S}_\mu \cdot \tilde{\mathbf{A}} \cdot \mathbf{S}_e - \mathcal{M}_\mu \cdot \mathbf{B} - \mathcal{M}_e \cdot \mathbf{B}$$

$$\tilde{\mathbf{A}} = \begin{pmatrix} A_\perp & 0 & 0 \\ 0 & A_\perp & 0 \\ 0 & 0 & A_\parallel \end{pmatrix}$$

$$A_\perp = A_{\rm iso} + D$$

$$A_\parallel = A_{\rm iso} - 2\,D$$

$$A = A_{\rm iso} + \frac{D}{2}(3\cos^2\theta - 1)$$

VOLUME 40, NUMBER 20 PHYSICAL REVIEW LETTERS 15 MAY 1978

Anomalous Muonium in Silicon

B. D. Patterson, A. Hintermann,[a] W. Kündig, P. F. Meier, and F. Waldner
Physics Institute, University of Zurich, Zurich, Switzerland

and

H. Graf, E. Recknagel, A. Weidinger, and Th. Wichert
Physics Department, University of Konstanz, Konstanz, Germany

(Received 21 February 1978)

The anomalous muonium state in Si has been studied with the muon-spin rotation technique as a function of the strength and orientation of the applied magnetic field. It was found that this state is well described by a spin Hamiltonian with axial symmetry about a [111] axis.

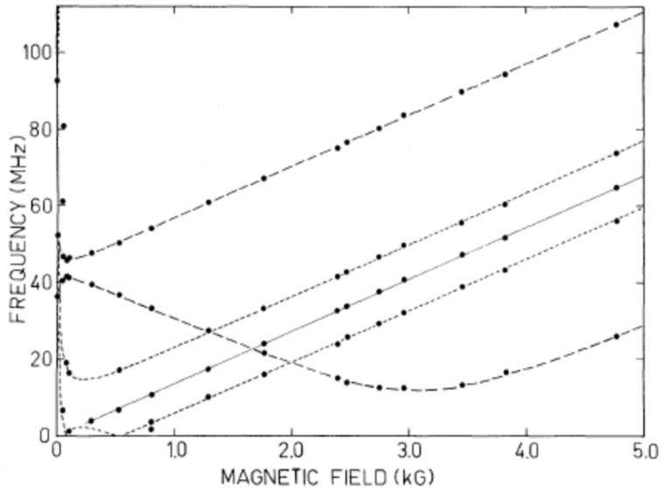

FIG. 2. The experimentally observed precession frequencies are plotted (solid circles) as a function of the external field applied along the [111] direction. Theoretical curves are included for the "μ^+" component (solid line) and for the "Mu*" components. The light (heavy) broken curves correspond to Mu* centers whose symmetry axes make an angle $\theta = 0°$ ($\theta = 70.5°$) with the applied field. The precession components attributable to "normal" muonium (Mu) are not shown.

The first μSR scoop: bond-centred Mu in Si (*et al.*)

SFJ Cox and MCR Symons,
Chem. Phys. Lett. **126**, 516 (1986)

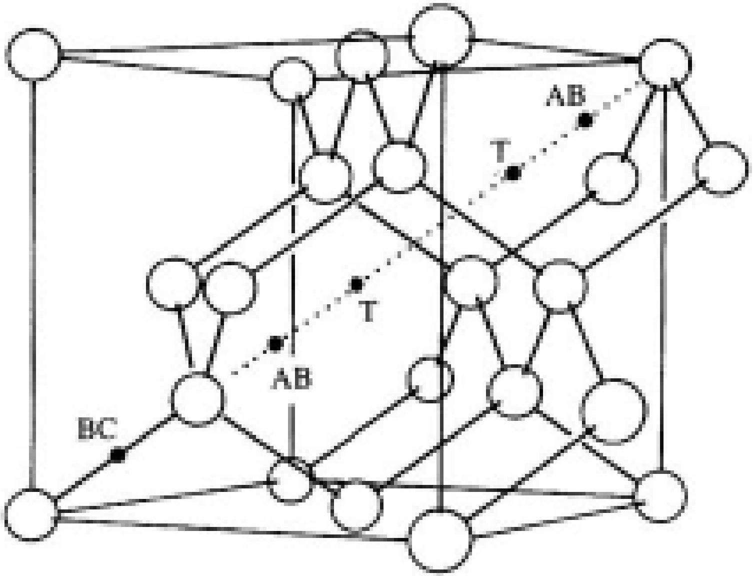

VOLUME 60, NUMBER 3 PHYSICAL REVIEW LETTERS 18 JANUARY 1988

^{29}Si Hyperfine Structure of Anomalous Muonium in Silicon: Proof of the Bond-Centered Model

R. F. Kiefl[a] and M. Celio
TRIUMF, Vancouver, British Columbia, Canada V6T 2A3

T. L. Estle
Rice University, Houston, Texas 77251

S. R. Kreitzman, G. M. Luke, and T. M. Riseman
University of British Columbia, Vancouver, British Columbia, Canada V6T 1W5

and

E. J. Ansaldo
University of Saskatchewan, Saskatoon, Saskatchewan, Canada S7N 0W0
(Received 21 August 1987)

The ^{29}Si hyperfine structure of the anomalous muonium center in silicon has been resolved in muon-spin-rotation spectra. The spectra of the weak ^{29}Si satellite lines show that there are two equivalent Si neighbors on the ⟨111⟩ symmetry axis with large positive *p*-like spin densities. These results, which are confirmed by level-crossing-resonance spectroscopy, establish that anomalous muonium in the group-IV semiconductors is an interstitial muonium located at the bond center.

PACS numbers: 71.55.Eq, 76.70.− r, 76.75.+i

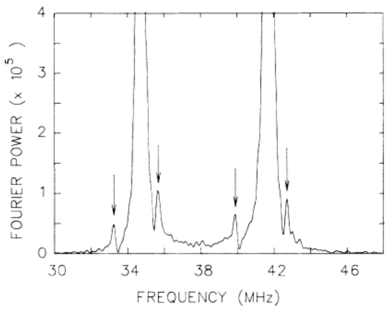

FIG. 1. The muon frequency spectrum in Si with a field 23.5 mT aligned along a ⟨100⟩ crystal direction. The small sa ellite lines, indicated by arrows, are due to Mu* centers whi have one nearest-neighbor ^{29}Si on the ⟨111⟩ symmetry ax For presentation clarity the time-differential data were ap dized prior to Fourier transformation in order to reduce t ringing from the strong main lines.

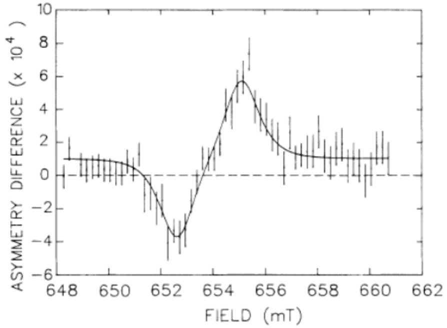

FIG. 3. The high-field level-crossing resonance for Mu* in silicon for those centers whose symmetry axes are at 90° to the field. The resonance occurs at a field where the muon transition frequency is matched to that of a ^{29}Si nearest neighbor (Ref. 11).

We now have a rather complete model for Mu/H in Si

B. Hitti et al., Phys. Rev. B **59**, 4918 (1999)

Configurations (including detailed microscopic characterization with hyperfine interaction)

- donor sitting at BC
- acceptor sitting at interstitial site

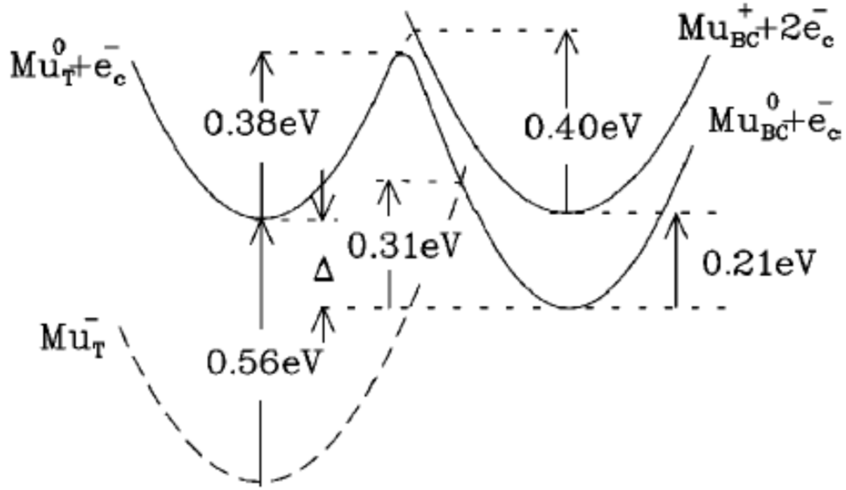

Donor and acceptor levels

Dynamics

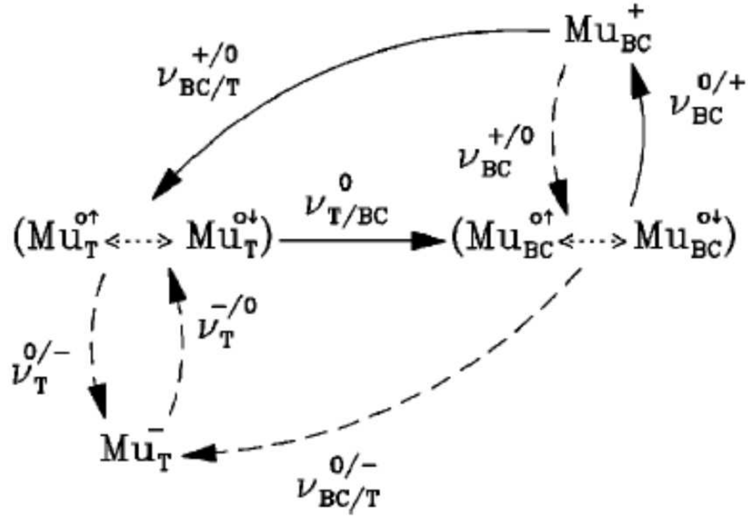

Don’t overinterpret every relaxing diamagnetic signal: it may just be some left-over from the implantation process...

PHYSICAL REVIEW B **96**, 195205 (2017)

Role of the transition state in muon implantation

R. C. Vilão,[1,*] R. B. L. Vieira,[1] H. V. Alberto,[1] J. M. Gil,[1] and A. Weidinger[2]
[1]*CFisUC, Department of Physics, University of Coimbra, P-3004-516 Coimbra, Portugal*
[2]*Helmholtz-Zentrum Berlin für Materialien und Energie, 14109 Berlin, Germany*
(Received 11 July 2017; published 16 November 2017)

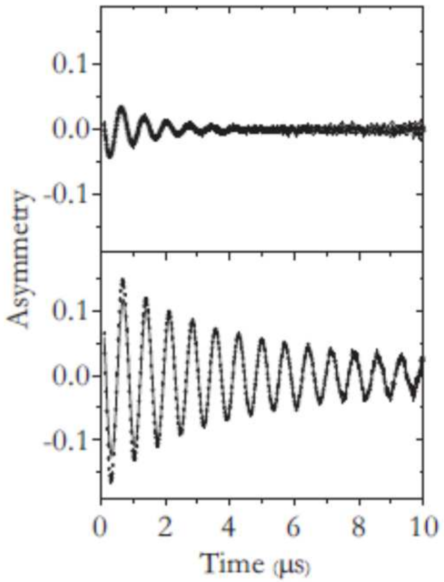

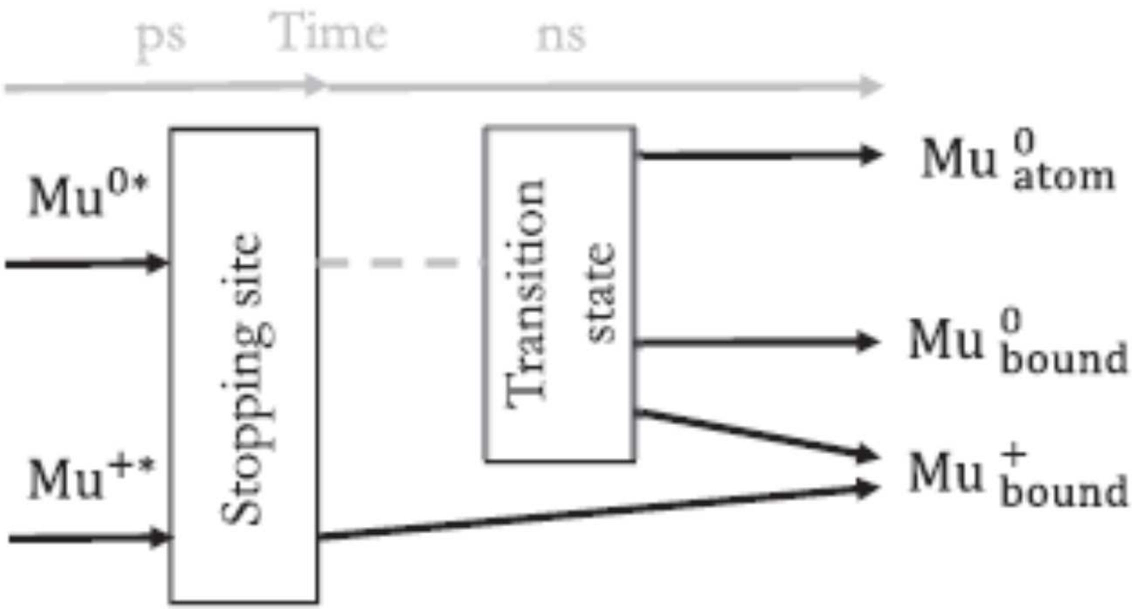

2 c) Complementarity to other methods

How do μSR results for isolated H in Si compare to other methods?

Sites and hyperfine interaction: available from ab-initio calculations only

Levels: available from macroscopic capacitance-voltage and deep-level transient spectroscopy experiments on silicon diodes

Method	E(0/+)	E(-/0)
Muon implantation	0.21 eV [Kre95]	$<$ 0.56 eV [Hit99]
Proton implantation	0.16 eV [Hol91]	0.65 eV [Bon02]
Dissociation of P-H complexes [Her01]	0.16 eV	0.67 eV
First-principles calculations [VdW89]	0.2 eV	0.6 eV

What about electron spin resonance in hydrogen? (EPR/ENDOR)

p^+/μ^+ Zeeman

e^- Zeeman

H/Mu ($p^+/\mu^+ e^-$) hyperfine

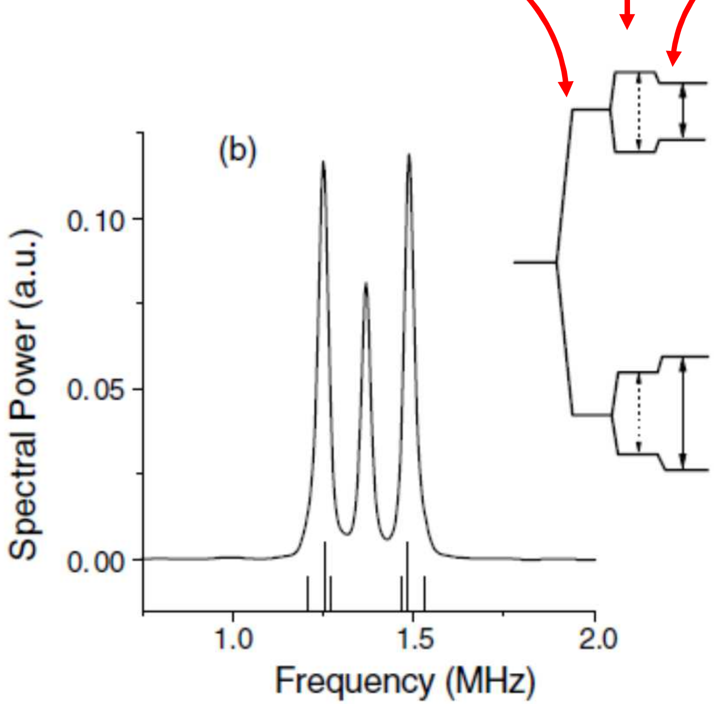

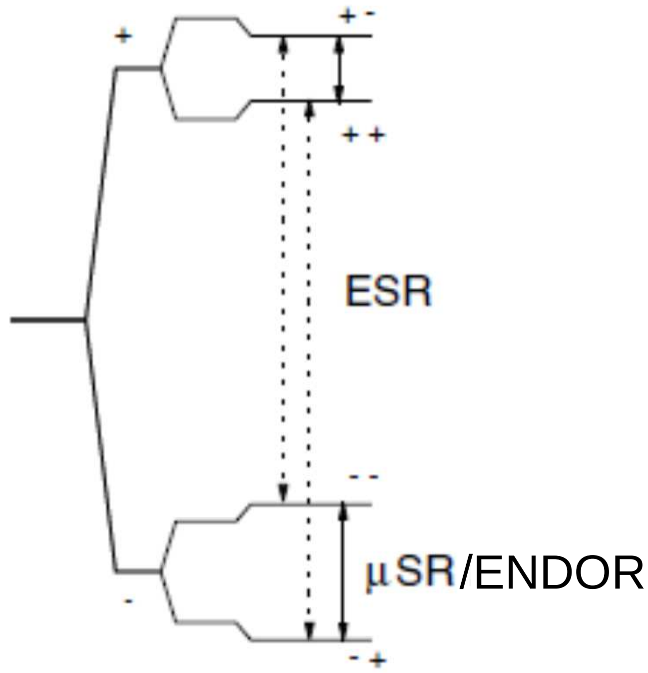

But... High concentration of isolated hydrogen required.
Hyperfine interaction for hydrogen by EPR/ENDOR determined only for ZnO and TiO_2

Overlapping local data for H/Mu I: ZnO

VOLUME 85, NUMBER 5 PHYSICAL REVIEW LETTERS 31 JULY 2000

Hydrogen as a Cause of Doping in Zinc Oxide

Chris G. Van de Walle*
Fritz-Haber-Institut der Max-Planck-Gesellschaft, Faradayweg 4-6, D-14 195 Berlin-Dahlem, Germany, and Paul-Drude-Institut, Hausvogteiplatz 5-7, D-10117 Berlin, Germany
(Received 3 February 2000)

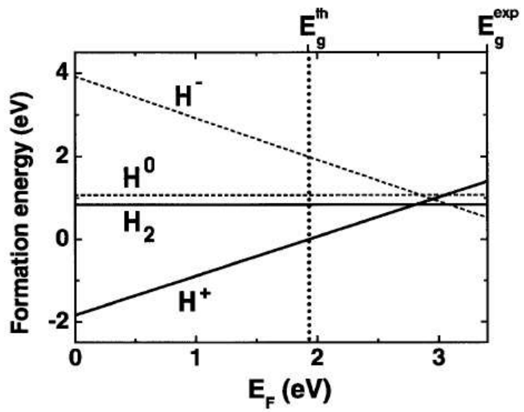

FIG. 2. Formation energies of interstitial hydrogen in ZnO, as a function of Fermi level, obtained from DFT-LDA calculations and referenced to the energy of a free H_2 molecule. For each charge state, only the lowest-energy configuration is shown. Zero-point energies are included. The zero of Fermi energy is chosen at the top of the valence band, and both the *theoretical* (E_g^{th} = 1.91 eV, dotted line) and *experimental* (E_g^{exp} = 3.4 eV) band gaps are indicated. The energies for H^0 and H^- are shown in dashed lines to indicate they are underestimated in the LDA calculations; after correction, H^+ is the lowest-energy state throughout the experimental band gap.

VOLUME 86, NUMBER 12 PHYSICAL REVIEW LETTERS 19 MARCH 2001

Experimental Confirmation of the Predicted Shallow Donor Hydrogen State in Zinc Oxide

S. F. J. Cox,[1,2] E. A. Davis,[3] S. P. Cottrell,[1] P. J. C. King,[1] J. S. Lord,[1] J. M. Gil,[4] H. V. Alberto,[4] R. C. Vilão,[4] J. Piroto Duarte,[4] N. Ayres de Campos,[4] A. Weidinger,[5] R. L. Lichti,[6] and S. J. C. Irvine[7]
[1]*ISIS Facility, Rutherford Appleton Laboratory, Chilton OX11 0QX, United Kingdom*
[2]*Department of Physics and Astronomy, University College London, London WCE 6BT, United Kingdom*
[3]*Department of Physics and Astronomy, University of Leicester, Leicester LEI 7RH, United Kingdom*
[4]*Physics Department, University of Coimbra, P-3004-516 Coimbra, Portugal*
[5]*Hahn-Meitner Institut Berlin, Glienicker Strasse 100, D-14109 Berlin, Germany*
[6]*Physics Department, Texas Tech University, Lubbock, Texas 79409-1051*
[7]*Chemistry Department, University of Wales, Bangor, Gwynedd LL57 2UW, United Kingdom*
(Received 10 October 2000)

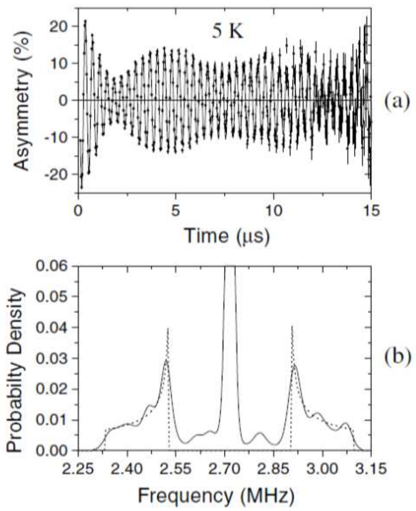

FIG. 1. (a) Muon spin rotation signal recorded for ZnO powder in 20 mT, below the ionization régime for the shallow donor state. (b) Maximum entropy frequency transform. The two broad distributions on either side correspond to the powder spectrum of the hyperfine-split lines. The dashed line is the expected frequency distribution for A_{iso} = 500 kHz and D = 260 kHz.

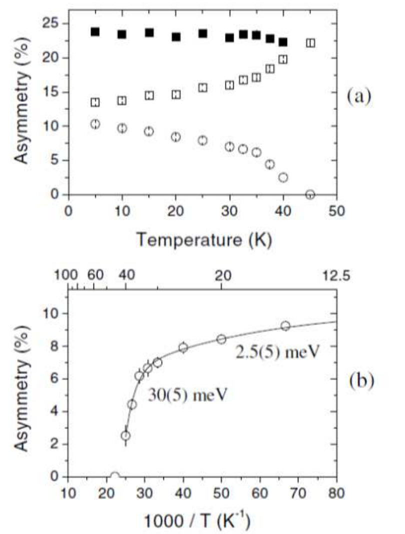

FIG. 2. (a) Amplitudes of the Larmor precession signal (open squares) and satellite lines (open circles), corresponding, respectively, to diamagnetic and paramagnetic states. The sum of these is approximately constant (filled squares). (b) Arrhenius plot for disappearance of the paramagnetic signal.

Overlapping local data for H/Mu I: ZnO

PHYSICAL REVIEW B, VOLUME 64, 075205

Shallow donor muonium states in II-VI semiconductor compounds

J. M. Gil, H. V. Alberto, R. C. Vilão, J. Piroto Duarte, and N. Ayres de Campos
Physics Department, University of Coimbra, P-3004-516 Coimbra, Portugal

A. Weidinger and J. Krauser
Hahn-Meitner Institut Berlin, Glienicker Strasse 100, D-14109 Berlin, Germany

E. A. Davis
Department of Physics and Astronomy, University of Leicester, Leicester LE1 7RH, United Kingdom

S. P. Cottrell
ISIS Facility, Rutherford Appleton Laboratory, Chilton OX11 0QX, United Kingdom

S. F. J. Cox
ISIS Facility, Rutherford Appleton Laboratory, Chilton OX11 0QX, United Kingdom
and Physics Department, University College London, London WCE 6BT, United Kingdom

(Received 8 February 2001; published 26 July 2001)

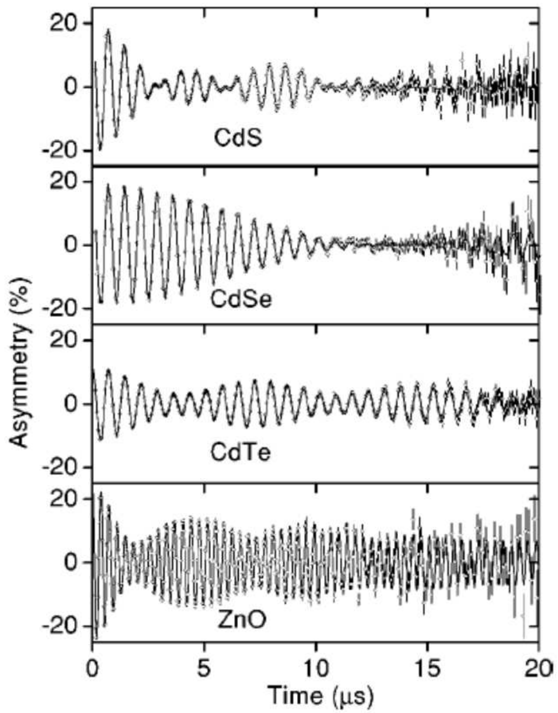

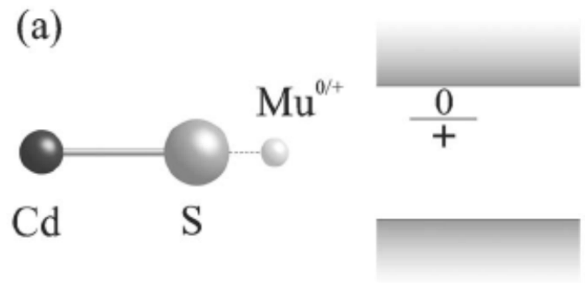

Shallow donor muonium states in II-VI semiconductors: another μSR scoop

Overlapping local data for H/Mu I: ZnO

VOLUME 88, NUMBER 4 PHYSICAL REVIEW LETTERS 28 JANUARY 2002

Hydrogen: A Relevant Shallow Donor in Zinc Oxide

Detlev M. Hofmann, Albrecht Hofstaetter, Frank Leiter, Huijuan Zhou, Frank Henecker, and Bruno K. Meyer
I. Physikalisches Institut, Heinrich-Buff-Ring 16, Justus-Liebig-Universität Giessen, D-35392 Giessen, Germany

Sergei B. Orlinskii and Jan Schmidt
Huygens Laboratory, Leiden University, P.O. Box 9504, 2300 RA Leiden, The Netherlands

Pavel G. Baranov
A. F. Ioffe Physico-Technical Institute, RAS, 194021 St. Petersburg, Russia
(Received 20 June 2001; published 10 January 2002)

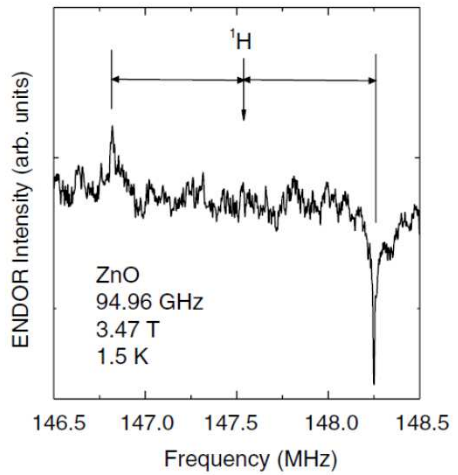

FIG. 4. The ENDOR spectrum of H of the *D*1 donor in ZnO. The conditions are the same as Fig. 3 (crystal *c* axis parallel to the static magnetic field).

A_{iso} (H)=1.4 MHz

VOLUME 86, NUMBER 12 PHYSICAL REVIEW LETTERS 19 MARCH 2001

Experimental Confirmation of the Predicted Shallow Donor Hydrogen State in Zinc Oxide

S. F. J. Cox,[1,2] E. A. Davis,[3] S. P. Cottrell,[1] P. J. C. King,[1] J. S. Lord,[1] J. M. Gil,[4] H. V. Alberto,[4] R. C. Vilão,[4] J. Piroto Duarte,[4] N. Ayres de Campos,[4] A. Weidinger,[5] R. L. Lichti,[6] and S. J. C. Irvine[7]

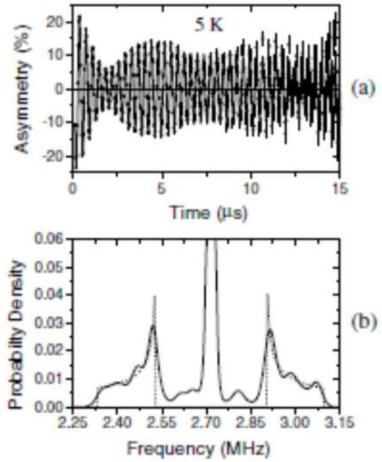

FIG. 1. (a) Muon spin rotation signal recorded for ZnO powder in 20 mT, below the ionization régime for the shallow donor state. (b) Maximum entropy frequency transform. The two broad distributions on either side correspond to the powder spectrum of the hyperfine-split lines. The dashed line is the expected frequency distribution for A_{iso} = 500 kHz and D = 260 kHz.

Experimental:
A_{iso} (Mu)= 0.5 MHz

Expected: A_{iso} (Mu)=3.183 A_{iso} (H)= 4.5 MHz

Different states? Is EPR/ENDOR observing a complex?

Overlapping local data for H/Mu II: TiO_2

ENDOR

AT Brant et al., J. App. Phys. **110**, 053714 (2011)

$A_1 = 0.616$ MHz
$A_2 = -\ 0.401$ MHz

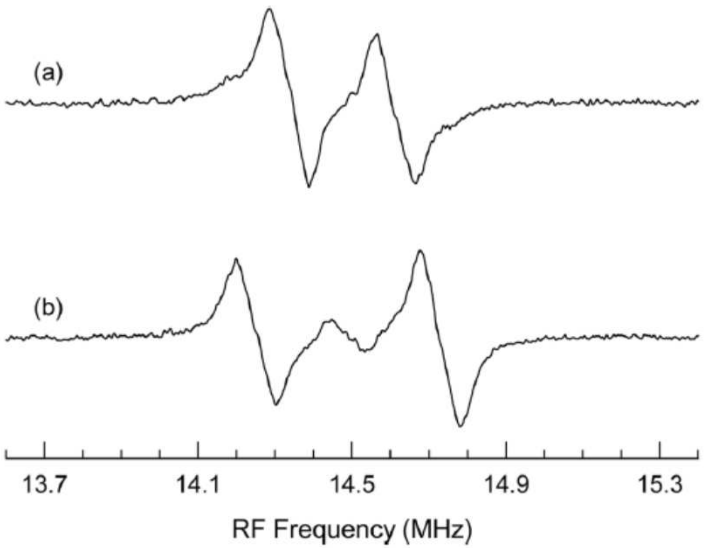

FIG. 7. ENDOR spectra from the neutral hydrogen donor taken at 5 K with the magnetic field parallel to the [100] direction. (a) ENDOR spectrum taken from the low-field EPR line. (b) ENDOR spectrum taken from the high-field EPR line.

bra

h

μSR

RC Vilão et al., Phys. Rev. B **92**, 081202(R) (2015)

Consistent with (ENDOR× 3.183)

$A_1 = 1.96$ MHz
$A_2 = -\ 1.28$ MHz

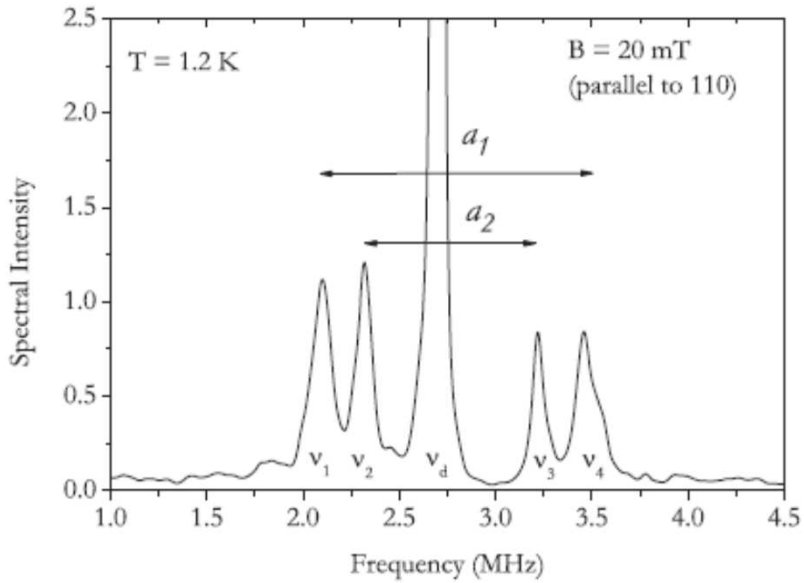

Local information from other techniques

Infrared vibrational spectroscopy

F. Bekisli et al.,
PRB **86**, 155208 (2012)

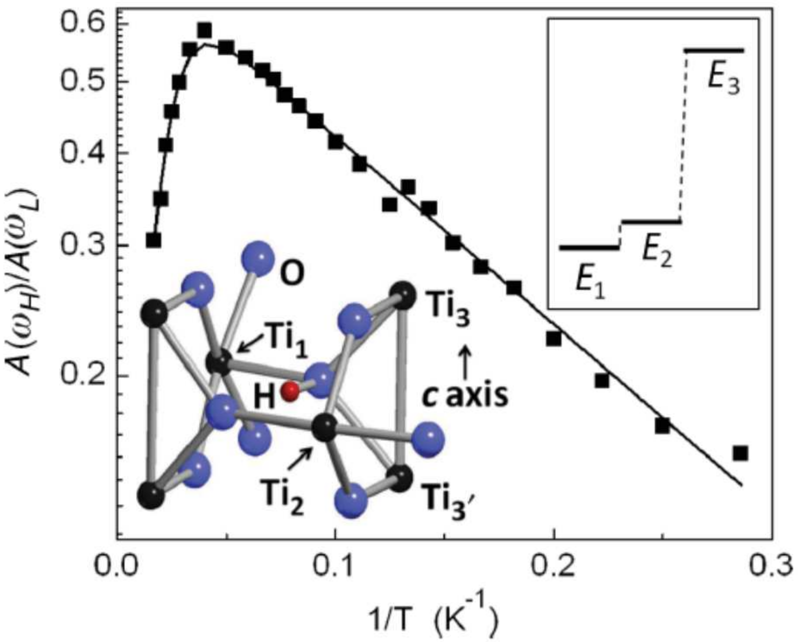

^{1}H Nuclear magnetic resonance

M. Wang *et al.*,
Chem. Phys. Lett. **627**, 7 (2015)

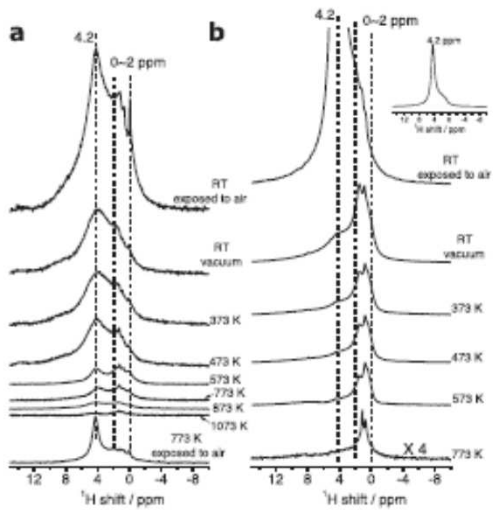

Figure 2. (a) Ambient temperature ^{1}H MAS NMR spectra of bulk ZnO exposed to air at RT, bulk ZnO exposed to vacuum at RT and different temperatures as well as bulk ZnO heated at 773 K then exposed to air. (b) ^{1}H MAS NMR spectra of as-prepared ZnO nanoparticles at RT and ZnO nanoparticles exposed to vacuum at RT and different temperatures. The inset shows the entire spectrum of as-prepared ZnO nanoparticles at RT. Note the spectral intensities in (a) are scaled 3 times larger than that of (b).

2 d) Hydrogen/Mu levels

PHYSICAL REVIEW B **84**, 045201 (2011)

Hydrogen impurity in paratellurite α-TeO_2: Muon-spin rotation and *ab initio* studies

R. C. Vilão,* A. G. Marinopoulos, R. B. L. Vieira, A. Weidinger, H. V. Alberto, J. Piroto Duarte,† and J. M. Gil
CEMDRX, Department of Physics, University of Coimbra, P-3004-516 Coimbra, Portugal

J. S. Lord and S. F. J. Cox
ISIS Facility, Rutherford Appleton Laboratory, Chilton, Didcot, Oxon OX11 0QX, United Kingdom
(Received 25 February 2011; revised manuscript received 4 May 2011; published 1 July 2011)

We present a systematic study of isolated hydrogen in α-TeO_2 (paratellurite) by means of muon-spin spectroscopy measurements complemented by *ab initio* calculations based on density-functional theory (DFT). The observable metastable states accessible by means of the muon implantation allowed us to probe both the donor and the acceptor configurations of hydrogen, as well as to follow their dynamics. A shallow donor state with an ionization energy of 6 meV as well as a deep acceptor state are proposed, together with their atomic-level configurations and associated formation energies obtained from the DFT calculations. The latter show a tendency of interstitial hydrogen to bind strongly to bridging oxygen ions but also to coexist at sites deeper in the interior of the Te–O–Te rings with a more atomiclike character and a defect level in the gap. Atomlike interstitial muonium was observed; it has a hyperfine interaction of about 3.5 GHz. Charge and site changes with temperature are discussed.

DOI: 10.1103/PhysRevB.84.045201 PACS number(s): 71.55.Ht, 71.15.Nc, 61.72.−y, 76.75.+i

1. Changes in asymmetry

Phenomenological Boltzmann functions

$$f_{\text{fast}}(T) = \frac{1}{2}\frac{f_p}{1 + N_1 \exp(-E_1/k_B T)},$$

$$f_{\text{slow}}(T) = \frac{f_p N_1 \exp(-E_1/kT)}{1 + N_1 \exp(-E_1/k_B T)} + f_d,$$

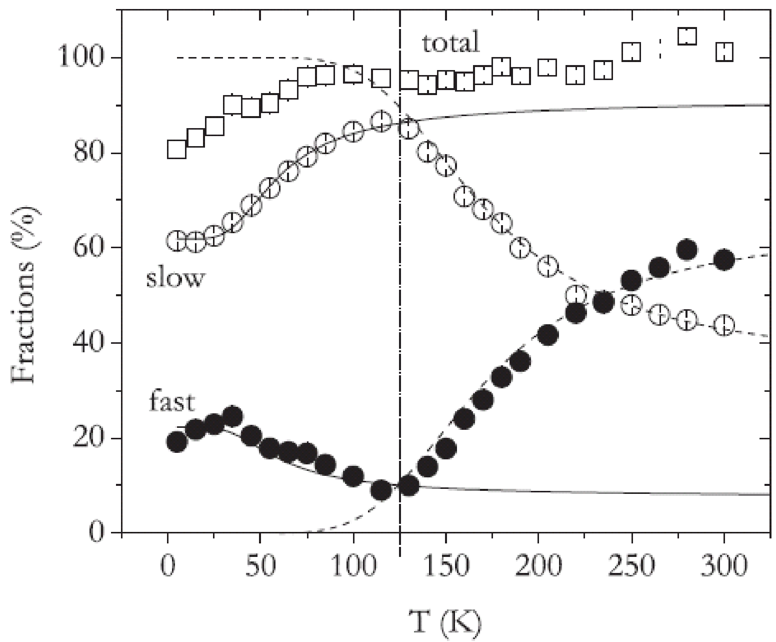

2 d) Hydrogen/Mu levels

PHYSICAL REVIEW B **72**, 235203 (2005)

Muonium spectroscopy in ZnSe: Metastability and conversion

R. C. Vilão,* H. V. Alberto, J. Piroto Duarte, J. M. Gil, A. Weidinger, and N. Ayres de Campos
Physics Department, University of Coimbra, P-3004-516 Coimbra, Portugal

R. L. Lichti
Physics Department, Texas Tech University, Lubbock, Texas 79409-1051, USA

K. H. Chow
Department of Physics, University of Alberta, Edmonton, Canada T6G 2J1

S. F. J. Cox
ISIS Facility, Rutherford Appleton Laboratory, Chilton, Didcot, Oxon OX11 0QX, United Kingdom
and Condensed Matter Physics, University College London, WC1E 6BT, United Kingdom
(Received 7 July 2005; revised manuscript received 14 September 2005; published 14 December 2005)

2. Conversion between Mu states: a simple approach

$$Mu_1 \underset{\lambda}{\longrightarrow} Mu_2$$

$$dP_1 = -\lambda P_1 \, dt \qquad P_1(t) = P_1^0 \exp(-\lambda t)$$

$$\begin{aligned}
\Delta P(t) &= P_{\rm I} \exp(-t/\tau) \cos(\omega_{\rm I} t) \\
&+ \frac{P_{\rm I}}{\sqrt{1+(\Delta\omega\,\tau)^2}} \cos(\omega_{\rm II} t - \tan^{-1}(\Delta\omega\,\tau)) \\
&- \frac{P_{\rm I} \exp(-t/\tau)}{\sqrt{1+(\Delta\omega\,\tau)^2}} \cos(\omega_{\rm I} t - \tan^{-1}(\Delta\omega\,\tau))
\end{aligned}$$

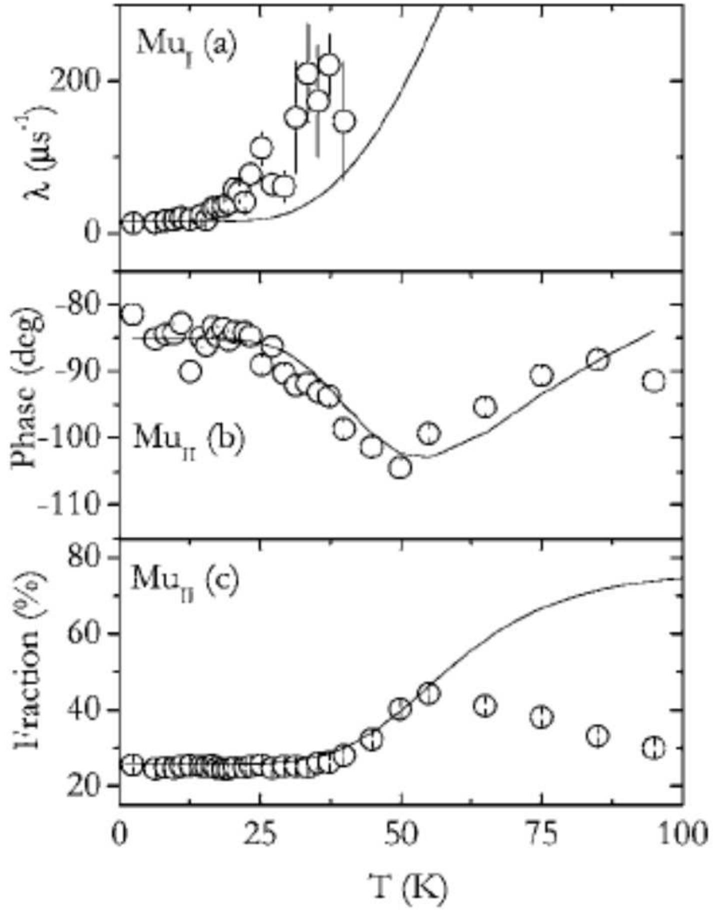

PRL 101, 136403 (2008) PHYSICAL REVIEW LETTERS week ending 26 SEPTEMBER 2008

Hydrogen Defect-Level Pinning in Semiconductors: The Muonium Equivalent

R. L. Lichti,[1,*] K. H. Chow,[2] and S. F. J. Cox[3,4]
[1]Department of Physics, Texas Tech University, Lubbock, Texas 79409-1051, USA
[2]Department of Physics, University of Alberta, Edmonton T6G 2G7, Canada
[3]STFC ISIS Facility, Rutherford Appleton Laboratory, Chilton OX11 0QX, United Kingdom
[4]Condensed Matter and Materials Physics, University College London, London WC1E 6BT, United Kingdom
(Received 15 June 2008; published 24 September 2008)

We have determined locations for the donor and acceptor levels of muonium in six semiconductor materials (Si, Ge, GaAs, GaP, ZnSe, and 6H-SiC) as a test of defect-level pinning for hydrogen. Within theoretical band alignments, our results indicate a common energy for the equilibrium charge-transition level Mu(+/−) to within experimental uncertainties. However, this is nearly 0.5 eV higher than the energy at which the equivalent level for hydrogen was predicted to be pinned. Corrections for zero-point energy account for only about 10% of this difference. We also report experimental results for the (negative-*U*) difference between donor and acceptor levels for Mu to be compared with calculated values for H impurities in the same materials.

DOI: 10.1103/PhysRevLett.101.136403 PACS numbers: 71.55.−i, 61.72.S−, 76.75.+i

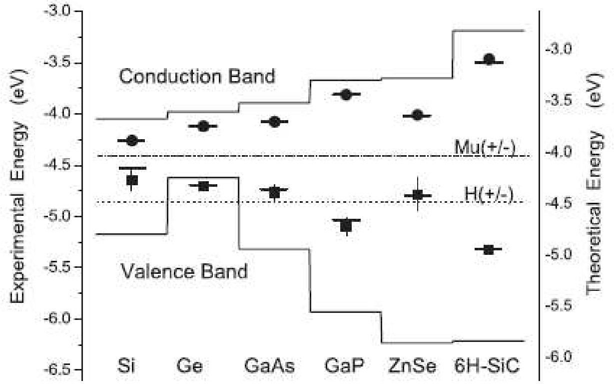

FIG. 2. Results for Mu defect levels: upper bar is the donor and lower bar is the acceptor level for each material; points are measured single-site levels. The dot-dashed and dashed lines represent our result for Mu(+/−) and the theoretical H(+/−) level [2], respectively.

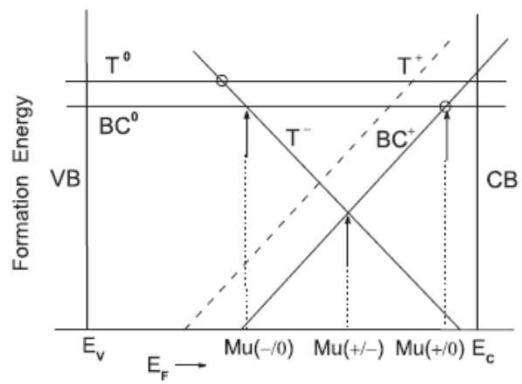

FIG. 1. Formation energies for stable and metastable Mu centers in cubic semiconductors as a function of E_F. Vertical arrows mark the Mu defect levels; circles mark experimentally accessible points; the dashed line is for the T_V donor site in III-V compounds.

2 e) Muon diffusion

PHYSICAL REVIEW B VOLUME 20, NUMBER 3 1 AUGUST 1979

Zero- and low-field spin relaxation studied by positive muons

R. S. Hayano, Y. J. Uemura, J. Imazato, N. Nishida, T. Yamazaki, and R. Kubo
Department of Physics, University of Tokyo, Bunkyo-ku, Tokyo, Japan
and TRIUMF, Vancouver, Canada
(Received 27 February 1979)

Zero- and low-field spin-relaxation functions have been studied for the first time by using positive muons, and results are compared with the stochastic theory of low-field relaxation formulated by Kubo and Toyabe. The dipolar broadening of the zero-field relaxation has been studied in detail. In ZrH_2, the zero-field relaxation function of μ^+ has been found to decay $(5)^{1/2}$ times faster than the high-field relaxation function, which is explained in terms of the contribution of the nonsecular part of the dipolar interaction. Advantages of the zero-field method over the conventional muon-spin rotation method in practical applications, especially for studies of the μ^+ diffusion/trapping, are discussed.

ZF: Kubo-Toyabe relaxation

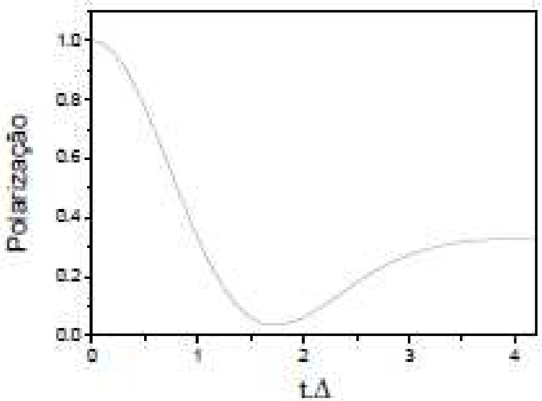

$$P(t) = \frac{1}{3} + \frac{2}{3}\left(1 - \Delta^2 t^2\right)\exp\left(-\frac{1}{2}\Delta^2 t^2\right)$$

oimbra

roach

2.3 Muon diffusion

2.3.1 TF: cosine with Abragam relaxation

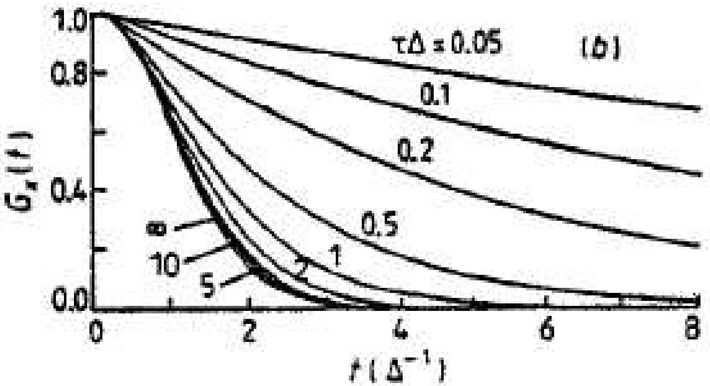

$$P(t) = \exp\left(-\frac{\sigma^2}{\nu^2}\left\{e^{-\nu t} - 1 + \nu t\right\}\right)\cos(\omega t)$$

2.3.2 ZF: Dynamical Kubo-Toyabe relaxation

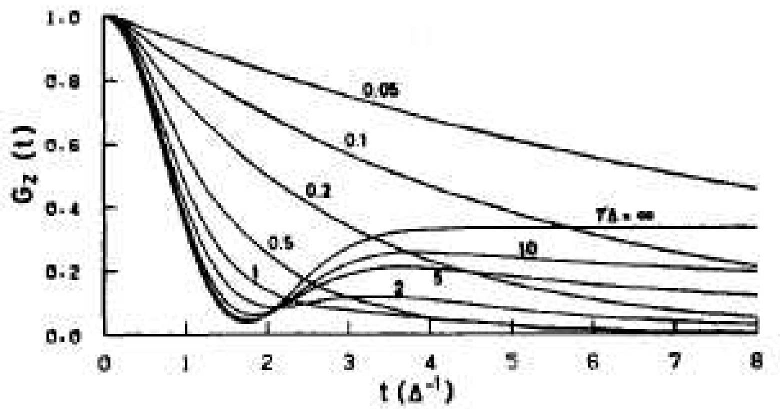

$$P(t) = KT_{stat}(t)e^{-\nu t} + \nu\int_{t'=0}^{t} e^{-\nu(t-t')}KT_{stat}(t-t')e^{-\nu t'}KT_{stat}(t')dt' + \ldots$$

3. Probing other defects: a) hydrogen passivation

Passivation of impurities

VOLUME 87, NUMBER 21 PHYSICAL REVIEW LETTERS 19 NOVEMBER 2001

Muonium Analog of Hydrogen Passivation: Observation of the Mu^+-Zn^- Reaction in GaAs

K. H. Chow,[1] B. Hitti,[2] R. F. Kiefl,[2,3] R. L. Lichti,[4] and T. L. Estle[5]
[1]*Department of Physics, University of Alberta, Edmonton, Alberta, Canada T6G 2J1*
[2]*TRIUMF, 4004 Wesbrook Mall, Vancouver, Canada V6T 2A3*
[3]*Canadian Institute for Advanced Research, University of British Columbia, Vancouver, Canada V6T 1Z1*
[4]*Department of Physics, Texas Tech University, Lubbock, Texas 79409-1051*
[5]*Department of Physics and Astronomy, Rice University, Houston, Texas 77251-1892*
(Received 12 March 2001; published 1 November 2001)

We report direct detection of the formation and subsequent breakup of a complex containing positively charged muonium (Mu^+) and a substitutional Zn_{Ga} acceptor in heavily doped p-type GaAs:Zn. Mu^+ diffuses above 200 K with a hop rate $\nu = \nu_0 e^{-E_\nu/k_B T}$ where $\nu_0 = (7.7 \pm 2.0) \times 10^8$ s^{-1} and $E_\nu = 0.15(4)$ eV. Above 350 K, it forms the complex with a trapping radius of 500 ± 200 Å. The Mu-Zn complex breaks up above 550 K with a dissociation energy of 0.88(7) eV and prefactor of $(5 \pm 4) \times 10^{12}$ s^{-1}. Above 750 K, the cyclic reaction $Mu^+ \leftrightarrow Mu^0$ takes place.

DOI: 10.1103/PhysRevLett.87.216403 PACS numbers: 71.55.Eq, 66.30.Jt, 76.75.+i

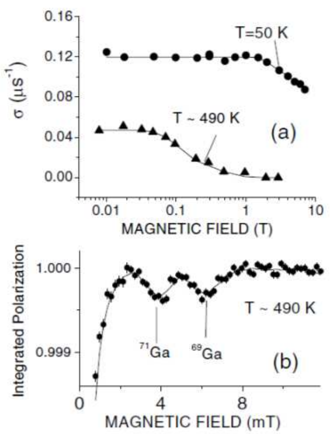

FIG. 3. (a) Transverse-field relaxation σ as a function of applied magnetic field for the isolated Mu^+ and the Mu-Zn complex. (b) μLCR spectrum of the Mu-Zn complex. The solid lines in both are guides to the eye.

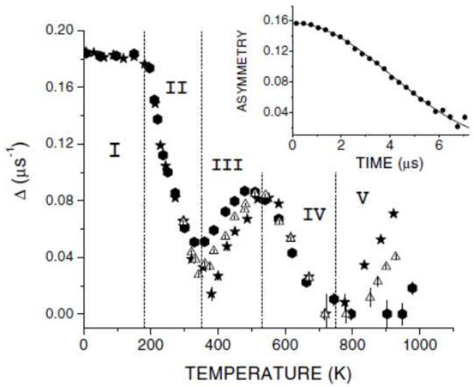

FIG. 1. Temperature dependence of the sKT relaxation rate Δ. The stars, open triangles, and closed hexagons correspond to GaAs-A, GaAs-B, and GaAs-C, respectively, The inset shows a typical zero-field spectrum (GaAs-A at 88 K). The solid line is a fit to the raw data using the sKT function.

Passivation of defects

Available online at www.sciencedirect.com
SCIENCE DIRECT
Physica B 326 (2003) 181–184
PHYSICA B
www.elsevier.com/locate/physb

Muon diffusion and trapping in chalcopyrite semiconductors

R.C. Vilão[a,*], J.M. Gil[a], H.V. Alberto[a], J. Piroto Duarte[a], N. Ayres de Campos[a], A. Weidinger[b], M.V. Yakushev[c], S.F.J. Cox[d,e]
[a] Physics Department, University of Coimbra, P-3004-516 Coimbra, Portugal
[b] Hahn-Meitner Institut Berlin, Glienicker Strasse, 100, D-14109 Berlin, Germany
[c] Department of Physics and Applied Physics, 107 Rottenrow, Strathclyde University, Glasgow G4 0NG, UK
[d] ISIS Facility, Rutherford Appleton Laboratory, Chilton, Didcot, Oxon OX11 0QX, UK
[e] Physics Department, University College London, WC1E 6BT, UK

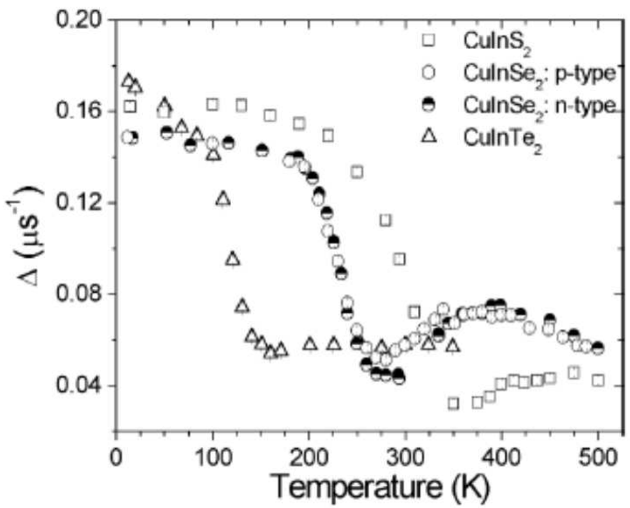

Fig. 1. Temperature dependence of the zero-field dipolar width Δ, measured on $CuInSe_2$ and $CuInTe_2$ single crystals and on $CuInS_2$ crystallites. The Δ values were obtained from fits of a single-component static KT function.

3. Probing other defects: b) defect layers in surfaces and junctions

PHYSICAL REVIEW MATERIALS **2**, 025402 (2018)

Slow-muon study of quaternary solar-cell materials: Single layers and *p*-*n* junctions

H. V. Alberto,[1,*] R. C. Vilão,[1] R. B. L. Vieira,[1] J. M. Gil,[1] A. Weidinger,[2] M. G. Sousa,[3] J. P. Teixeira,[3] A. F. da Cunha,[3] J. P. Leitão,[3] P. M. P. Salomé,[3,4] P. A. Fernandes,[3,4,5] T. Törndahl,[6] T. Prokscha,[7] A. Suter,[7] and Z. Salman[7]

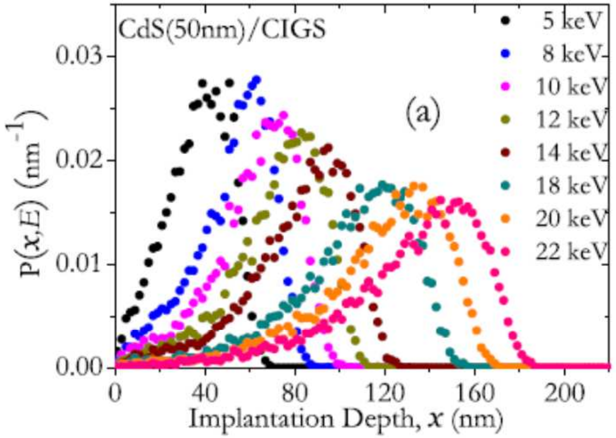

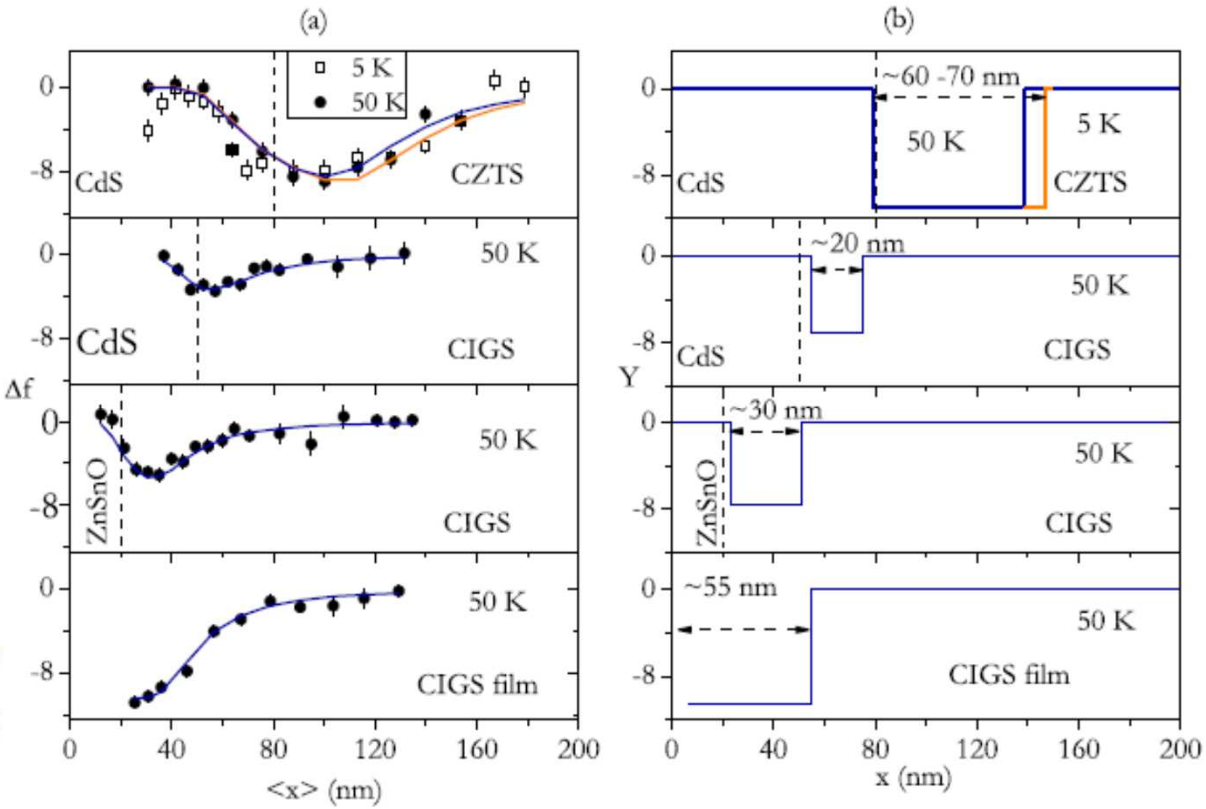

4. Addressing charge-carrier dynamics

Electrical activity: capture, loss and scattering of carriers

SFJ Cox,
ISIS Muon
Training Course
2008

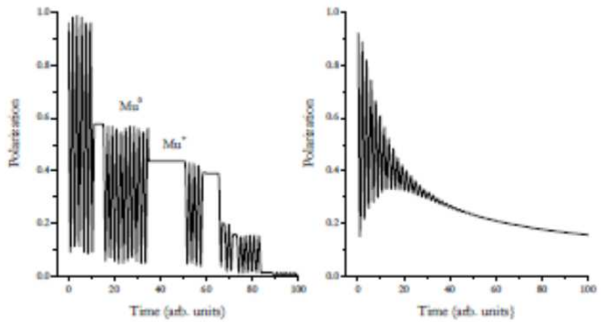

Charge exchange

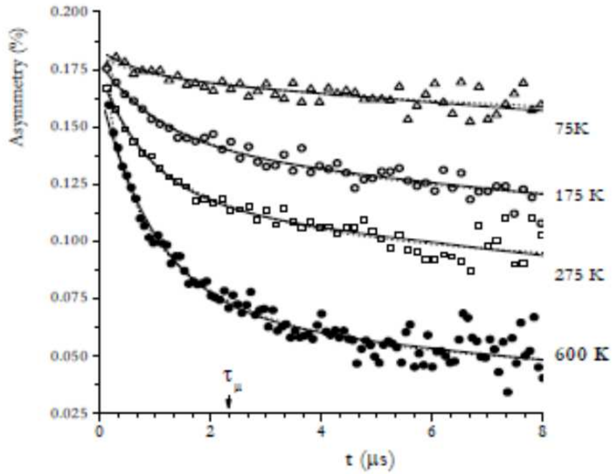

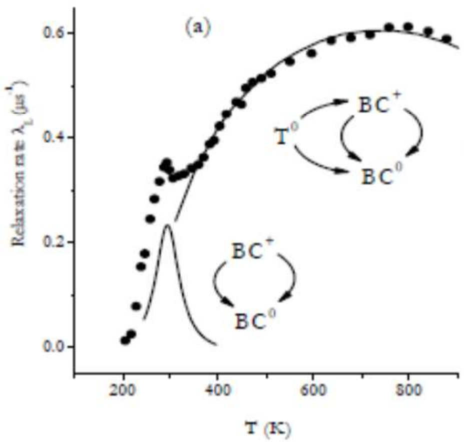

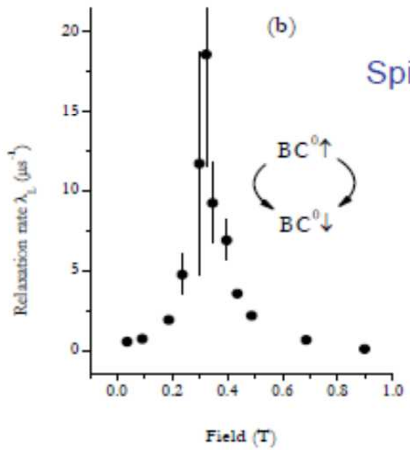

Spin exchange

Spin-charge exchange dynamics probed in longitudinal fields

$$Mu^0 \xrightarrow[\lambda_0]{} Mu^{\pm}$$

$$Mu^{\pm} \xrightarrow[\lambda_{\pm}]{} Mu^0$$

$$\frac{1}{T_1} = \frac{1}{2}\left(\frac{\lambda_0\,\lambda_{\pm}}{\lambda_0 + \lambda_{\pm}}\right)\left(\frac{\omega_0^2}{\lambda_0^2 + \omega_{24}^2}\right)$$

RAPID COMMUNICATIONS

PHYSICAL REVIEW B VOLUME 47, NUMBER 23 15 JUNE 1993-I

Muonium dynamics in Si at high temperatures

K. H. Chow, R. F. Kiefl, and J. W. Schneider
TRIUMF, 4004 Wesbrook Mall, Vancouver, British Columbia, Canada V6T 2A3

B. Hitti and T. L. Estle
Department of Physics, Rice University, Houston, Texas 77251-1892

R. L. Lichti
Department of Physics, Texas Tech University, Lubbock, Texas 79409-1051

C. Schwab
Centre de Recherches Nucléaires, F-67037 Strasbourg CEDEX, France

R. C. DuVarney
Department of Physics, Emory University, Atlanta, Georgia 30322

S. R. Kreitzman, W. A. MacFarlane, and M. Senba
TRIUMF, 4004 Wesbrook Mall, Vancouver, British Columbia, Canada V6T 2A3

(Received 21 January 1993)

We report longitudinal muon-spin-relaxation measurements in intrinsic Si from 350 to 850 K. The data are explained by a two-state model describing alternating charge states of muonium resulting from thermally excited electrons. Within this model, the average muon-electron hyperfine parameter in the neutral state is consistent with muonium at the tetrahedral interstitial site. This indicates that at the highest temperatures measured neutral muonium spends significant time away from the bond center site, the calculated adiabatic potential minimum.

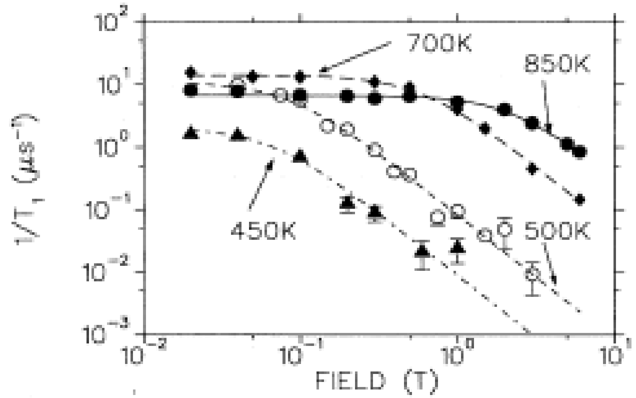

FIG. 2. The muon $1/T_1$ relaxation rate in nominally pure Si as a function of magnetic field. The curves are the best global fit to the charge-exchange model described in the text.

4. Measuring carrier recombination with photo-excited muSR

PRL 119, 226601 (2017) PHYSICAL REVIEW LETTERS week ending 1 DECEMBER 2017

Photoexcited Muon Spin Spectroscopy: A New Method for Measuring Excess Carrier Lifetime in Bulk Silicon

K. Yokoyama,[1,2,*] J. S. Lord,[2] J. Miao,[1,3] P. Murahari,[1] and A. J. Drew[1,2,3,†]
[1]*School of Physics and Astronomy, Queen Mary University of London, Mile End, London E1 4NS, United Kingdom*
[2]*ISIS, STFC Rutherford Appleton Laboratory, Didcot OX11 0QX, United Kingdom*
[3]*College of Physical Science and Technology, Sichuan University, Chengdu 610064, People's Republic of China*

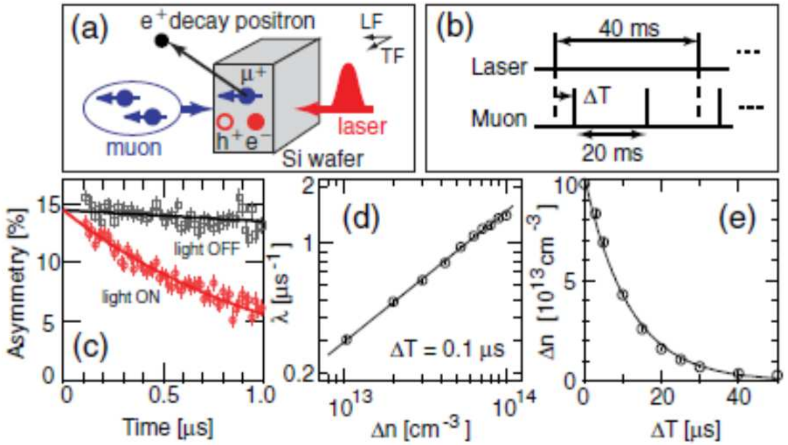

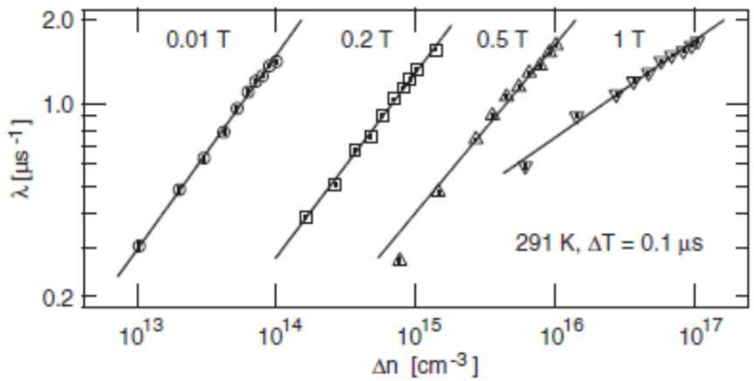

Conclusions

- Hydrogen as a relevant impurity in semiconductors
- Mu as a light pseudo-isotope of H
- μSR gives important and unique local information about electronic configurations of Mu/H, particularly through the hyperfine interaction
- Transition levels for isolated H can be determined
- Motion and interaction with other impurities/defects can also be adressed
- μSR can be used to probe defect layers and charge-carrier dynamics.

In short:

Anything hydrogen does, muonium does better!

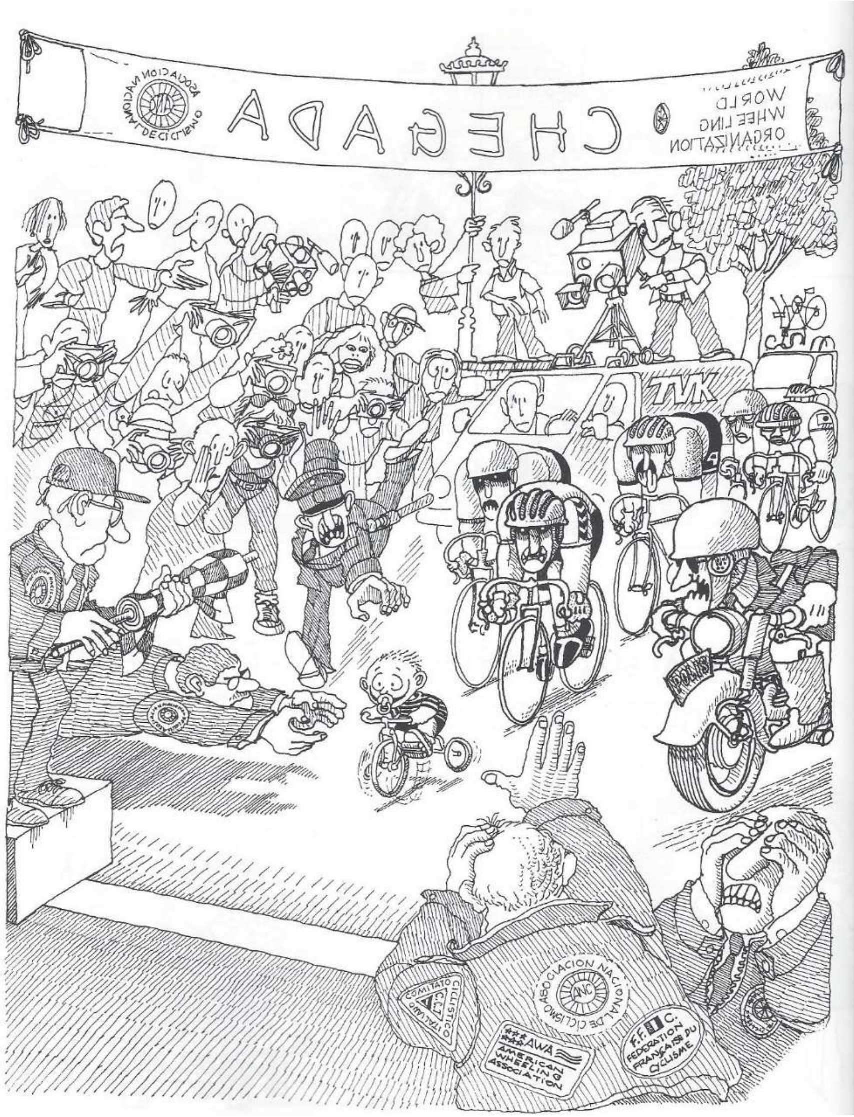

Appendix

Eigenstate	Eigenvectors (base $\|m_\mu\, m_e\rangle$)	Eigenenergy
$\|1\rangle$	$\|++\rangle$	$\frac{hA}{4} + \frac{h(\gamma_e - \gamma_\mu)B}{2}$
$\|2\rangle$	$\sin\zeta\|+-\rangle + \cos\zeta\|-+\rangle$	$-\frac{hA}{4} + \frac{h(\gamma_e+\gamma_\mu)\sqrt{B^2+B_0^2}}{2}$
$\|3\rangle$	$\|--\rangle$	$\frac{hA}{4} - \frac{h(\gamma_e - \gamma_\mu)B}{2}$
$\|4\rangle$	$\cos\zeta\|+-\rangle - \sin\zeta\|-+\rangle$	$-\frac{hA}{4} - \frac{h(\gamma_e+\gamma_\mu)\sqrt{B^2+B_0^2}}{2}$

Table 2.3: Isotropic muonium eigenvectors and eigenvalues corresponding to the Breit-Rabi hamiltonian 2.3. B_0 and the amplitudes of probability $\cos\zeta$ and $\sin\zeta$ are defined in equations 2.13 and 2.15.

$$\cos\zeta = \left(\frac{1+\frac{1}{2}\left(\frac{B_0}{B}\right)^2}{1+\left(\frac{B_0}{B}\right)^2}\right)^{\frac{1}{2}} = \left(\frac{2x^2+1}{2(x^2+1)}\right)^{\frac{1}{2}}$$

$$\sin\zeta = \left(\frac{\frac{1}{2}\left(\frac{B_0}{B}\right)^2}{1+\left(\frac{B_0}{B}\right)^2}\right)^{\frac{1}{2}} = \left(\frac{1}{2(x^2+1)}\right)^{\frac{1}{2}}$$

$$x = \frac{B}{B_0}$$

$$B_0 = \frac{A}{\gamma_e + \gamma_\mu}$$

$B_0 = 0.1585$ T in vacuum

Appendix

polarization $\vec{p}_\mu(t)$ of the muon spin ensemble

$$p_\mu(t) = \sum_{\mathrm{nm}} a_{\mathrm{nm}} \cos 2\pi\nu_{\mathrm{nm}} t$$

nm	a_{nm}	$\nu_{\mathrm{nm}} = \lvert E_{\mathrm{n}} - E_{\mathrm{m}}\rvert / h$
12	$(\cos\zeta)^2/2$	$\left\lvert \frac{A}{2} + \frac{(\gamma_e-\gamma_\mu)B}{2} - \frac{(\gamma_e+\gamma_\mu)\sqrt{B^2+B_0^2}}{2} \right\rvert$
34	$(\cos\zeta)^2/2$	$\left\lvert \frac{A}{2} - \frac{(\gamma_e-\gamma_\mu)B}{2} + \frac{(\gamma_e+\gamma_\mu)\sqrt{B^2+B_0^2}}{2} \right\rvert$
14	$(\sin\zeta)^2/2$	$\left\lvert \frac{A}{2} + \frac{(\gamma_e-\gamma_\mu)B}{2} + \frac{(\gamma_e+\gamma_\mu)\sqrt{B^2+B_0^2}}{2} \right\rvert$
23	$(\sin\zeta)^2/2$	$\left\lvert -\frac{A}{2} + \frac{(\gamma_e-\gamma_\mu)B}{2} + \frac{(\gamma_e+\gamma_\mu)\sqrt{B^2+B_0^2}}{2} \right\rvert$

Table 2.4: Isotropic muonium precession amplitudes and frequencies.